

# Design and Analysis of Mechanical and Electronic Subsystems of Electronic Continuously Variable Transmission

submitted in partial fulfilment of the requirements of the degree of

**'Bachelor of Engineering'**

by

Prathamesh Mehta	60005180077
Rishit Gandhi	60005180086
Sadique Selia	60005180090
Yash Thakkar	60005180126

Under Project Guide:

**Dr. Hari Vasudevan**



Department of Mechanical Engineering

Dwarkadas J. Sanghvi College of Engineering

University of Mumbai

2021-2022

## **CERTIFICATE**

This is to certify that the project entitled “**DESIGN AND ANALYSIS OF MECHANICAL AND ELECTRONIC SUBSYSTEMS OF ELECTRONIC CONTINUOUSLY VARIABLE TRANSMISSION**” is a bonafide work of

**PRATHAMESH MEHTA (60005180077)**

**RISHIT GANDHI (60005180086)**

**SADIQUE SELIA (60005180090)**

**YASH THAKKAR (60005180126)**

Submitted to the University of Mumbai in partial fulfilment of requirement for the award of the degree “**Bachelor of Engineering**” in “**Mechanical Engineering**”.

---

Project Guide

Dr. Hari Vasudevan

---

Head of the Department

Dr. K.N. Vijaya Kumar

---

Principal

Dr. Hari Vasudevan

## **Project Report Approval for B.E.**

This project report entitled "**DESIGN AND ANALYSIS OF MECHANICAL AND ELECTRONIC SUBSYSTEMS OF ELECTRONIC CONTINUOUSLY VARIABLE TRANSMISSION**"

*By*

**PRATHAMESH MEHTA (60005180077)**

**RISHIT GANDHI (60005180086)**

**SADIQUE SELIA (60005180090)**

**YASH THAKKAR (60005180126)**

is approved for the degree of **Bachelor of Engineering in Mechanical Engineering.**

Examines:

1. \_\_\_\_\_
2. \_\_\_\_\_

Date:

Place:

## **DECLARATION**

We declare that this written submission represents our ideas in our own words and where other's ideas or words have been included, we have adequately cited and referenced the original sources. We also declare that we have adhered to all the principles of academic honesty and integrity and have not misrepresented or fabricated or falsified any idea/data/fast/source in our submission. We understand that any violation of the above will be a cause for disciplinary action by the Institute and can also evoke penal action from the sources, which thus not been properly cited or from whom permission has not been taken, when needed.

---

**PRATHAMESH MEHTA**

**(60005180077)**

---

**RISHIT GANDHI**

**(60005180086)**

---

**SADIQUE SELIA**

**(60005180090)**

---

**YASH THAKKAR**

**(60005180126)**

Date:

Place:

## **ACKNOWLEDGEMENT**

The successful execution of this project would not have been possible without the guidance and unwavering support of our Project Guide and Principal, Dr. Hari Vasudevan of Dwarkadas J. Sanghvi College of Engineering and Head of Department, Dr. K. N. Vijaya Kumar of Mechanical Engineering. Their involvement in our project helped us to overcome the difficulties and challenges, we faced while working on our project, especially in these tough times of COVID-19.

Last but not the least; we would like to thank the entire Department of Mechanical Engineering, Dwarkadas J. Sanghvi College of Engineering for their patience and support throughout the course of the project.

---

**PRATHAMESH MEHTA**

**(60005180077)**

---

**RISHIT GANDHI**

**(60005180086)**

---

**SADIQUE SELIA**

**(60005180090)**

---

**YASH THAKKAR**

**(60005180126)**

Date:

## **ABSTRACT**

A continuously variable transmission commonly known as CVT is a type of automatic transmission in which the gear ratio changes automatically depending on the load on the vehicle. CVT is the optimum choice for fuel economy, good acceleration or when the terrain varies continuously (Eg: An All-Terrain Vehicle (ATV)). It is a mechanical component where the shifting of sheaves (pulley) is obtained by utilizing the rotational rpm of the CVT itself which is powered by the engine. Although it's possible, it is very difficult to achieve the accurate ratios as required by various terrain conditions. That is due to many variable factors such as centrifugal force, RPM, spring tension and ramp angles. Due to the various iterations, the tuning time and cost increases.

Hence, to overcome these difficulties and make the CVT more efficient, cost effective and increase the ease of use, an Electronically actuated CVT was designed. The following document outlines the design process, analysis and simulation of the electronically actuated continuously variable transmission (ECVT).

The mechanical design and control system was integrated into the custom designed mechanical transmission system created in parallel. The transmission was initially designed for use in Baja SAE vehicle but later was modified for general use. Through market research, operational requirements, previous and alternate CVT designs, and vehicle characteristics, we were able to determine the requirements and specifications for our unique system. Input, output, speed, and durability requirements guided our hardware selection.

The primary components which comprised our system include an alternator and regulator, optical speed sensors and hall effect sensors, stepper motors, lead screws, and a custom system enclosure; further details are included in this report. With the knowledge of our vehicle characteristics, actuation mode, and inputs, a system model determined that a standard proportional + integral + differential action (PID) controller would be sufficient to obtain the speed and accuracy demanded by our needs. The entire system is also realised in MATLAB Simulink to obtain the simulation for real life operation. In conjunction with controls specific setbacks, resulted in the final combined system remaining untested on the field, this project can continue to be tested and improved upon in future by real life testing and prototyping of the electronic system for more realistic gains and results.

## **CONTENT**

<b>CHAPTER</b>	<b>TITLE</b>	<b>PAGE NO.</b>
	Abstract	2
Chapter 1	Introduction	7
Chapter 2	Literature Review	16
Chapter 3	Design of CVT Parameters	19
Chapter 4	Methodology for Material Selection	23
Chapter 5	Design & Analysis of CVT Actuation Mechanism	26
Chapter 6	Design & Selection of Electronic Components	46
Chapter 7	Control System Concept Design Development	71
Chapter 8	Simulation	81
Chapter 9	Future Scope	84
	Conclusion	85
	References	86

## LIST OF FIGURES

<b>SR. NO.</b>	<b>FIG. NO.</b>	<b>DESCRIPTION</b>	<b>PAGE NO.</b>
1	1.1	CVT Sheave movements	7
2	1.2	Exploded view of ECVT	9
3	1.3	A Trapezoidal Power screw & nut assembly	10
4	1.4	Basic terms in limits and tolerances	11
5	1.5	Types of Fits	12
6	1.6	ESP32 Function Block Diagram	13
7	1.7	ESP32	13
8	1.8	PID controller logic flow	14
9	1.9	Exploded View of Stepper Motor	15
10	1.10	A Baja ATV	15
11	1.11	Baja Engine Power Curve	15
12	1.12	Baja Engine Torque Curve	16
13	3.1	CVT belt dimension	16
14	3.2	Primary Sheave dimensions	21
15	3.3	Secondary Sheave dimensions	22
16	3.4	Axial displacement of primary movable sheave	23
17	3.5	Axial displacement of secondary movable sheave	23
18	4.1	Hole basis system	26
19	4.2	Shaft basis system	26
20	5.1	E-CVT Primary Sheave Assembly	27
21	5.2	Force visualization of Primary Sheave Assembly	29
22	5.3	Primary Motor mount iteration 1	30
23	5.4	Primary Motor mount iteration 1 loading condition	31
24	5.5	Primary Motor mount iteration 1 analysis	31
25	5.6	Primary Motor mount iteration 2	31
26	5.7	Primary Motor mount iteration 2 loading condition	32
27	5.8	Primary Motor mount iteration 2 analysis	32
29	5.9	Fork and Nut assembly iteration 1	33
30	5.10	Fork and Nut assembly iteration 2	33
31	5.11	Fork and Nut assembly iteration 2 loading condition	34
32	5.12	Fork and Nut assembly iteration 2 analysis	34
33	5.13	Exploded view of primary CVT	35
34	5.14	Shaft of primary CVT analysis	35
35	5.15	Keyway adaptor of primary CVT analysis	36
36	5.16	Fixed sheave of primary CVT analysis	36
37	5.17	Movable sheave of primary CVT analysis	37
38	5.18	Force visualisation of integrated nut assembly	39
39	5.19	Sectional view of secondary sheave assembly	39

40	5.20	Secondary motor mount iteration 1	39
41	5.21	Secondary motor mount iteration 1 loading condition	40
42	5.22	Secondary motor mount iteration 1 analysis	40
43	5.23	Secondary motor mount iteration 2	40
44	5.24	Secondary motor mount iteration 2 analysis	41
45	5.25	Secondary Integrated Nut	41
46	5.26	Secondary Integrated Nut loading condition	42
47	5.27	Secondary Integrated Nut analysis	42
48	5.28	Secondary CVT exploded view	42
49	5.29	Shaft of Secondary CVT loading condition	43
50	5.30	Shaft of Secondary CVT analysis	43
51	5.31	Keyway adaptor of Secondary CVT loading condition	44
52	5.32	Keyway adaptor of Secondary CVT analysis	44
53	5.33	Sheaves of Secondary CVT Loading condition	44
54	5.34	Sheaves of Secondary CVT analysis	45
55	5.35	Optical RPM sensor mounts on primary and secondary CVT	45
56	5.36	Hall sensor mounts on primary and secondary CVT	45
57	6.1	Stepper Motor	47
58	6.2	Brushless DC motor	48
59	6.3	Brushed DC Motor	49
60	6.4	Linear Magnetic Actuator	50
61	6.5	Permanent Magnet Stepper Motor	51
62	6.6	Variable Reluctance Stepper Motor	52
63	6.7	Hybrid Type Stepper Motor	53
64	6.8	Unipolar Stepper Motor	56
65	6.9	Bipolar Stepper Motor	57
66	6.10	5618L-52P, NEMA 17	58
67	6.11	Torque Curve of 5618L-52P, NEMA 17	58
68	6.12	Arduino Nano RP 2040	60
69	6.13	Teensy 3.5	61
70	6.14	ESP32 S2	62
71	6.15	55505-00-02-A	64
72	6.16	SS-5GL13T-A12	65
73	6.17	13461 Contactless IR	66
74	6.18	Turnigy TGY-APD02	67
75	6.19	PTA6043-2015DPA103	68
76	6.20	Schematic Diagram	70
77	6.21	Circuit diagram of the Electrical system	71
78	7.1	Basic Proportional-Integral-Differential Controller Architecture	72
79	7.2	Fuzzy Logic Controller Architecture	73
80	7.3	Optimal Control and Full State Feedback	74
81	7.4	Baja Engine Power Curve	74

82	7.5	Ideal CVT Shift Curve	75
83	7.6	Neural Network Controller Model	75
84	7.7	PID Equation	76
85	7.8	Arduino Code Part 1	77
86	7.9	Arduino Code Part 2	78
87	7.10	Arduino Code Part 3	78
88	7.11	Python Code Iteration 1 Part 1	79
89	7.12	Python Code Iteration 1 Part 2	79
90	7.13	Python Code Iteration 1 Part 3	80
91	7.14	Python Code Iteration 2 Part 1	81
92	7.15	Python Code Iteration 2 Part 2	81
93	8.1	Modelling Ideology	82
94	8.2	Controller Subsystem	82
95	8.3	Plant Subsystem	83
96	8.4	MATLAB-BAJA Model	83
97	8.5	Primary and Secondary RPMs vs Speed (kmph)	84
98	8.6	CVT Ratio vs Vehicle Speed (kmph)	84

## LIST OF TABLES

<b>SR NO.</b>	<b>TABLE NO.</b>	<b>TABLE NAME</b>	<b>PAGE NO.</b>
1	4.1	Characteristics of various materials	25
2	4.2	Material selected for various components	25
3	6.1	Motor selection matrix	52
4	6.2	Stepper motor characteristics	59
5	6.3	Motor specifications	60
6	6.4	Operating specifications of motor	60
7	6.5	Microcontroller selection matrix	64
8	6.6	Pros and Cons of Embedded C/C++	64
9	6.7	Pros and Cons of MicroPython	65
10	6.8	Sensor List	70
11	7.1	Selection matrix for control algorithm	77

# CHAPTER 1

## INTRODUCTION

### **1.1 CONTINUOUSLY VARIABLE TRANSMISSION(CVT)**

A continuously variable transmission (CVT) is an automatic transmission that can change seamlessly through a continuous range of gear ratios. This contrasts with other transmissions that provide a limited number of gear ratios in fixed steps. The flexibility of a CVT with suitable control may allow the engine to operate at a constant RPM while the vehicle moves at varying speeds.

A CVT achieves this infinite gear ratio flexibility by using two opposing cone-shaped pulleys with a chain or belt that runs between them. This setup is very similar to the way a chain operates across the gears of a bicycle. One cone is connected to the engine output shaft, while the other cone directs power to the driveshaft and drive wheels. Gear ratios change as the pulleys move closer and further apart, causing the chain or belt to move up and down the two cones' sides. This movement increases or decreases the diameter of the chain or belt, which alters the gear ratio based on the power needed. These real-time changes happen continually as the car is moving. CVT sheave movement is shown in Figure 1.1

The CVT can be tuned to ensure that it engages at the torque peak of the engine and it starts shifting out at the power peak of the engine. This will result in the engine staying at the power peak resulting in maximum acceleration. The tuning of a mechanical CVT depends on various factors such as the roller weights, ramp angle, primary spring stiffness in the primary pulley and the helix angle and secondary spring stiffness in the secondary pulley.

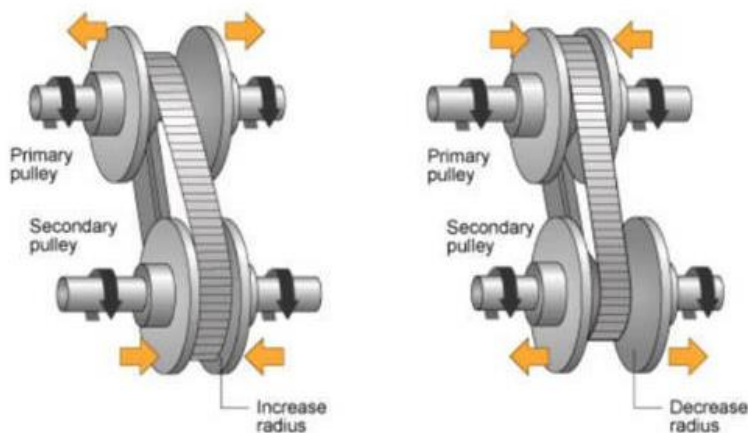


Figure 1.1: CVT Sheave movements

## **1.2 PROS & CONS OF A CVT**

### Pros:

- Improved fuel economy: CVTs are more efficient than standard automatic transmissions and are commonly utilized in hybrid powertrains and smaller cars to maximize the number of kilometres you can travel on every litre of fuel.
- Responsive Acceleration: Due to its variable characteristics, a CVT can typically find the proper gear ratio much faster than an automatic transmission at virtually every speed ranging from off-the-line to highway passing.
- Smoother driving character: The absence of hard shift points means a CVT delivers more consistent performance across the engine's rev band. There are no abrupt downshifts or lags in acceleration as experienced with automatic and manual transmissions.

### Cons:

- Lack of character: There is little to no shifting feel which results in a driving experience that can be bland and uninteresting.
- Noisiness: Many drivers find CVTs to be louder and whinier than traditional automatic transmissions. Under hard acceleration, such as when entering a freeway, they tend to drone. This trait contributes to a less enjoyable driving character.
- Lack of high-performance capability and durability: Although CVTs offer better than average acceleration in everyday driving situations, they are not ideal for high horsepower applications or sustaining high speeds. For that reason, CVTs are typically not utilized in sports cars.
- Higher repair costs: Not only do CVTs cost more to fix or replace, they generally do not last as long as traditional automatic transmissions.

## **1.3 NEED FOR AN ELECTRONICALLY ACTUATED CVT (E-CVT)**

With an E-CVT, we have the following advantages:

- Increased cost effectiveness.
- Simple and compact design with decreased number of components.
- Lower heat loss and higher overall efficiency.
- Improved user experience as live tuning will be possible by altering the various constants of the actuation mechanism therefore resulting in a lot of customization.

## 1.4 COMPONENTS OF E-CVT

The E-CVT can be divided into two sub-systems: mechanical sub system and electronic sub system.

The mechanical subsystem consists of the following components:

- Trapezoidal power screw for conversion of rotation motion of stepper motor into linear motion for the sheave movement
- The power screw is connected to the fork assembly which will transmit the linear motion to the sheaves
- The fork assembly consists of the rollers which will actually be in contact with the sheave.

The electronic subsystem consists of the following components:

- The ESP32 micro computer which is the CPU of the entire system
- Stepper motors for actuation of CVT
- Hall effect sensors for determination of position of CVT sheaves
- IR sensor for measurement of various RPMS
- Potentiometer for throttle input

Exploded view of all components of electronic CVT is shown in 1.2

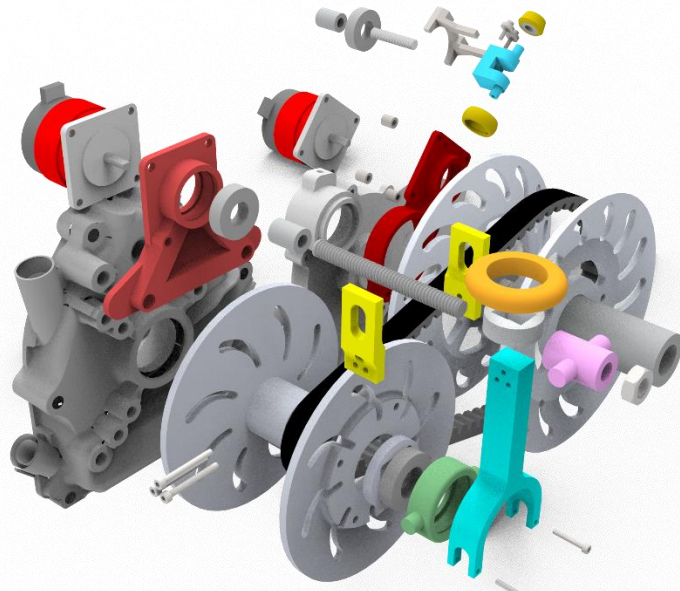


Figure 1.2: Exploded view of ECVT

## 1.5 TRAPEZOIDAL POWER SCREWS

Also known as a lead screw, A power screw is a mechanical component which is used to convert rotary motion into the linear motion. It uses helical motion of screw to transmit the power rather than holding the parts together. With suitably sized threads, they are capable of large mechanical advantage. A trapezoidal screw is shown in Figure 1.3.

Advantages of Power Screws:

- It has large load carrying capacity
- It can be designed with self-locking property.
- Compact, cost effective and reliable
- It gives smooth and noiseless service
- It requires almost no maintenance
- Its manufacturing is easy and does not require any specialized machinery
- It is simple to design

Disadvantages of Power Screws:

- It has poor efficiency
- Due to high friction, wear is a serious problem in power screws

In our application, the Power screw is connected to the stepper motor to convert the rotary motion of the stepper motor to linear motion of the fork which transmits it to the sheaves



Figure 1.3: A Trapezoidal Power screw & nut assembly

## 1.6 FITS & TOLERANCES

Along with the tolerances, fits are important. Giving a loose fit may cause sliding between the mating parts. Too tight a fit between the mating parts may impose unnecessary loads which may cause failure very soon. Hence limits and fits are very important while designing an E-CVT. The three types of Fits are namely: Interference, Transition and Clearance Fit. Various terms in limits and tolerances are shown in Figure 1.4.

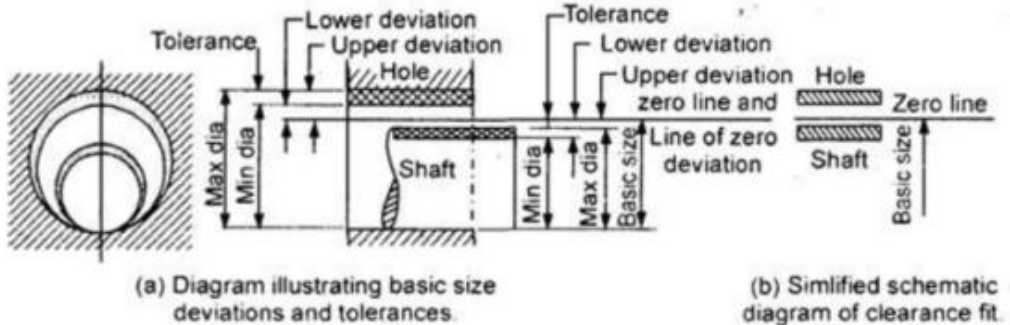


Figure 1.4: Basic terms in limits and tolerances

**Upper Deviation:** The algebraic difference between the maximum limit of size (of either hole or shaft) and the corresponding basic size, like  $ES$ ,  $es$ .

**Lower Deviation:** The algebraic difference between the minimum limit of size (of either hole or shaft) and the corresponding basic size, like  $EI$ ,  $ei$ .

**Fundamental Deviation:** It is one of the two deviations which is chosen to define the position of the tolerance zone.

**Tolerance:** The algebraic difference between upper and lower deviations. It is an absolute value.

**Limits of Size:** There are two permissible sizes for any particular dimension between which the actual size lies, maximum and minimum.

**Basic Shaft and Basic hole:** The shafts and holes that have zero fundamental deviations. The basic hole has zero lower deviation whereas, the basic shaft has zero upper deviation.

### 1.6.1 Types of Fits

The three types of fits are:

1. Clearance - The hole is larger than the shaft, enabling the two parts to slide and / or rotate when assembled.
2. Transition - The hole is fractionally smaller than the shaft and mild force is required to assemble / disassemble.

3. Interference - The hole is smaller than the shaft and high force and / or heat is required to assemble / disassemble.

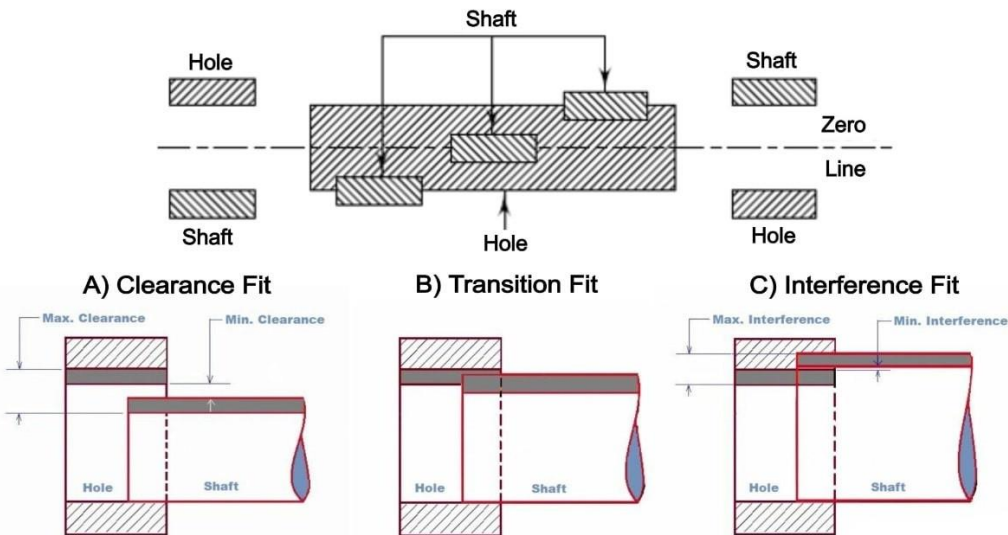


Figure 1.5: Types of Fits

## 1.7 ESP 32 MICRO CONTROLLER

Created by Espressif Systems, ESP32 is a low-cost, low-power system on a chip (SoC) series with Wi-Fi & dual-mode Bluetooth capabilities. At its heart, there's a dual-core or single-core Tensilica Xtensa LX6 microprocessor with a clock rate of up to 240 MHz. Engineered for mobile devices, wearable electronics, and IoT applications, ESP32 achieves ultra-low power consumption through power saving features including fine resolution clock gating, multiple power modes, and dynamic power scaling. We are using ESP32 as the micro controller for the entire electronic subsystem of our product

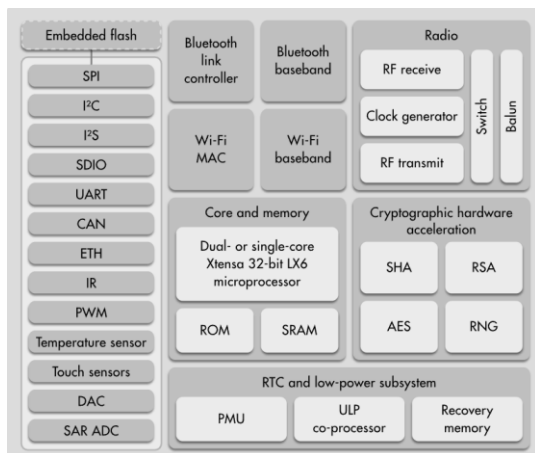


Figure 1.6: ESP32 Function Block Diagram

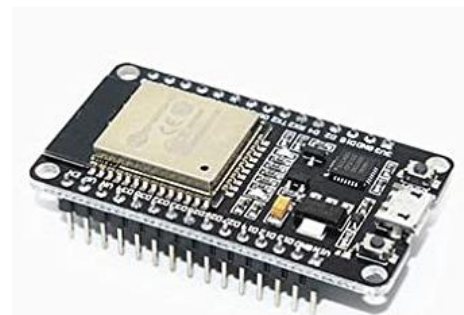


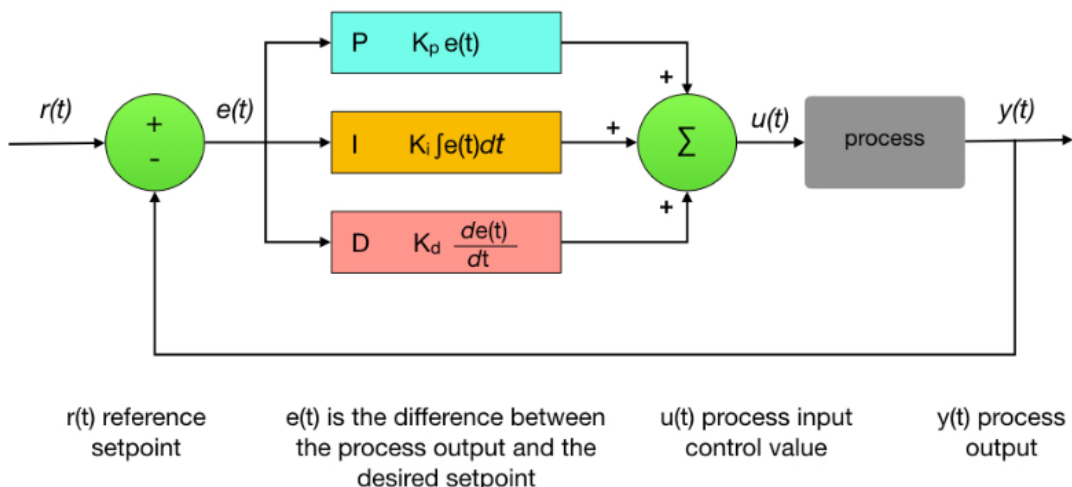
Figure 1.7: ESP32

## 1.8 PID

A PID controller is an instrument used in industrial control applications to regulate temperature, flow, pressure, speed and other process variables. PID (proportional integral derivative) controllers use a control loop feedback mechanism to control process variables and are the most accurate and stable controller.

PID control is a well-established way of driving a system towards a target position or level. It's a practically ubiquitous as a means of controlling temperature and finds application in myriad chemical and scientific processes as well as automation. PID control uses closed-loop control feedback to keep the actual output from a process as close to the target or setpoint output as possible.

In our project, the PID controller logic is used to perform the tuning of CVT. The PID is programmed to ensure that the engine rpm remains at its power peak and it achieves this by varying the reduction ratio of the CVT based on the information it receives from the various sensors in the subsystem. The constants of the PID logic are adjusted based on the characteristic performance desired from the CVT.



## 1.9 STEPPER MOTOR

A stepper motor is an electromechanical device it converts electrical power into mechanical power. Also, it is a brushless, synchronous electric motor that can divide a full rotation into an expansive number of steps. The motor's position can be controlled accurately without any feedback mechanism, as long as the motor is carefully sized to the application. Stepper motors are similar to switched reluctance motors.

The stepper motor uses the theory of operation for magnets to make the motor shaft turn a precise distance when a pulse of electricity is provided. The stator has eight poles, and the rotor has six poles. The rotor will require 24 pulses of electricity to move the 24 steps to make one

complete revolution. Another way to say this is that the rotor will move precisely  $15^\circ$  for each pulse of electricity that the motor receives.

The stepper motor is used as an actuator for the power screw. The ESP32 micro controller is what provides the instructions to the motor

Advantages of a stepper motor:

- Simple construction and it works in any situation.
- Compatible digital systems.
- Flexibility and provides a constant holding torque without the need for the motor to be powered.
- Stepper motors are safer.
- Stepper motors are very reliable and have low accuracy.
- Excellent response to starting and stopping.
- Different kinds of rotational speeds by which we can realize as the speed is proportional to the frequency of the input pulses.

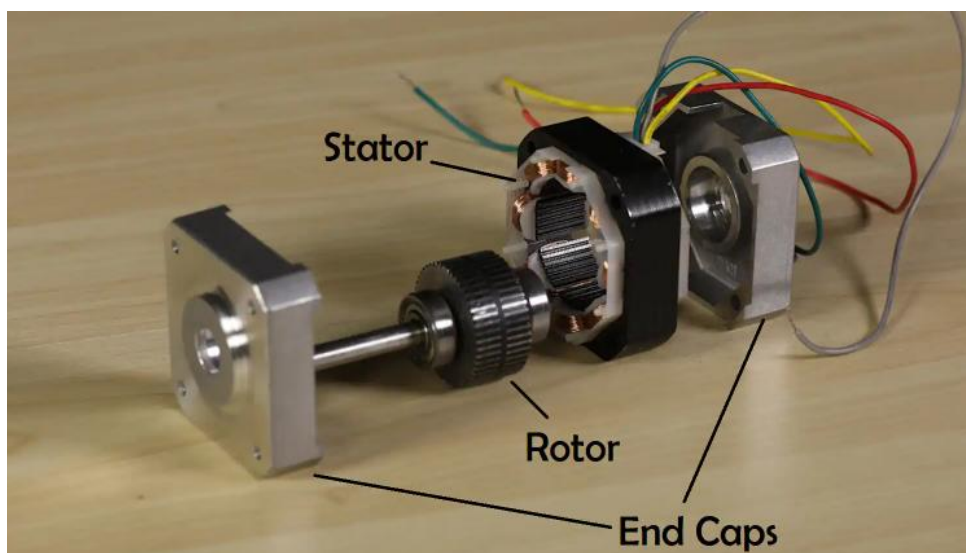


Figure 1.9: Exploded View of Stepper Motor

## 1.10 ALL TERRAIN VEHICLE

An all-terrain vehicle (ATV), also known as a quad, quad bike, three-wheeler, and four-wheeler is a vehicle that is designed to go on any Terrain or any obstacle that comes in front it. Many events of off-road Racing are conducted across India. Baja SAE INDIA is conducted every year in the month of January. The type of Off-Road vehicle is known as Baja. These vehicles use Briggs & Stratton 305cc 8HP Engine driven Reduction Gearbox. For such vehicles, high torque is required as opposed to speed.

The E-CVT we have designed is based on the Baja ATV. The calculations are done based on that Briggs & Stratton engine which has its torque peak at 2800 rpm and power peak at 3600 rpm



Figure 1.10: A Baja ATV

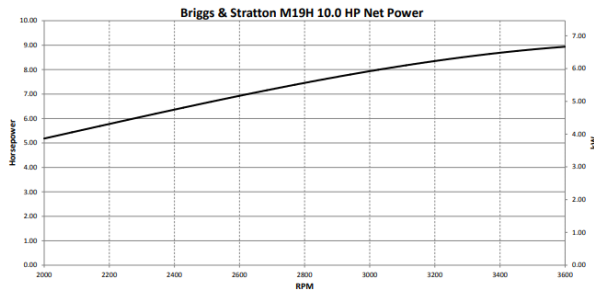


Figure 1.11: Baja Engine Power Curve

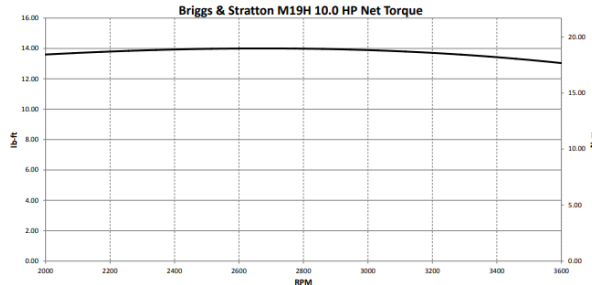


Figure 1.12: Baja Engine Torque Curve

## **CHAPTER 2**

### **LITERATURE REVIEW**

Dong, Jian et al. [8] In this paper, a review of the state-of-the-art of various CVT powertrain systems now used or being planned for future use in HEVs was presented. These CVT powertrain systems were classified into three main categories: mechanical CVT, electromechanical CVT (ECVT) and pure electrical CVT (EVT). The research development, system architecture, operation characteristics and the merits and drawbacks of each type are discussed. This paper was the inspiration behind the project and highlight the issues with the different system of CVTs currently in use in the industry. The team have spend various session in discussing the differences in CVTs and finally decided upon ECVT as the best of the three.

Supriyo et al. [1] introduced an electro-mechanical, dual acting pulley, continuously variable transmission (EMDAPCVT) and presented its real time ratio controller using a proportional-derivative-plus-conditional-integral (PDPCI) controller. The ratio controller system developed based on primary (input) and secondary (output) pulley position controllers. Each position controller has two PID parameters, releasing and clamping, which were determined experimentally using a relay feedback method. A PC-based ratio controller system was implemented using Matlab/Simulink® software and a Keithley DAS-1602 data acquisition system card. The experimental results showed that the PDPCI controller system can control the CVT ratio adequately. This gave us an outline of how the controller systems are applied with a nonlinear system like the ECVT.

Seelan [2] helped to understand the contribution of Hydraulic Actuators. Furthermore, the question of how and why a Torque Converter has effectively replaced a conventional clutch has been answered. The materials used, constructional aspects and stress analysis of the belt has been discussed in detail. Recent developments in clamping force control for the push belt Continuously Variable Transmission (CVT) have resulted in increased efficiency in combination with improved robustness. Current control strategies attempt to always prevent macro slip between elements and pulleys for maximum robustness. This helped to assess the possibilities of using hydraulic actuation as a viable option for our version of ECVT.

Ryu [3] proposed a modified CVT ratio map to obtain the improved fuel economy for a metal belt CVT. Since the CVT system loss, which occupies most of the drivetrain loss, depends on the engine speed, input torque, primary and secondary actuator pressure, a modified CVT ratio map was produced to realize the highest engine-CVT overall efficiency through the consideration of CVT system loss. The modified CVT ratio map was constructed with respect to the demanded vehicle power and present vehicle speed based on the steady state CVT system loss. Using the modified CVT ratio map, performance simulations were carried out using the dynamic models of the CVT powertrain. This paper provided insights for the mathematical foundation and derived the ratio map wrt engine characteristics.

Aulakh, Deepinder [4] Presented work aimed to develop Genetic Algorithm (GA) based simulation approach for tuning of Continuously Variable Transmission (CVT). This study used force balance to model the behaviour of CVT in MATLAB and employed dual level GA to optimize the tuning variables for desired output from CVT i.e. engagement of belt and sheaves at peak of engine torque curve, start of shifting at peak of engine power curve and keeping constant engine RPM (peak of power curve) during shifting. Also, the behaviour of CVT tuned by simulation is compared with the traditional method of experimental .This study concluded with strong confidence in the potential of GA simulations for tuning. This paper was referenced as to explore the working of Genetic Algorithm in the tuning operation but this approach was later disregarded as the working of GA required historic data for every optimization and in addition its efficacy wrt non linear system makes it less robust for the application.

Xie, F [6] stated comparison of control effects of PID control and fuzzy control, this dissertation designed hybrid ratio tracking controller combining the advantages of both PID and fuzzy control. Using MATLAB/Simulink, simulation research of typical working conditions was made, such as start-up, acceleration and ramp driving. The results showed that the controller has strong capacity of robust and decoupling and good dynamic response and high accuracy control of steady state, and good dynamic stability under the resistance of outside environment. During the brainstorming session, two schools of thoughts prevailed in the team and thus this paper helped to take clear stand for the issue.

Akehurst, S., et al. [7] in this paper an overview of CVTs operating by traction through small contact areas is performed, the layouts and kinematics of leading examples are reviewed, including the factors affecting design optimization. Properties of the traction contacts are considered in detail, with particular attention to elastic-hydrodynamic lubrication and asperity contact. Factors affecting the traction coefficient are reviewed and fundamental empirical predictions are contrasted with modern modelling computations, this paper helped to understand the motion of belt and corresponding force analysis to track the trajectory of the belt across the operation cycle and better understand the motion of the sheaves for tuning.

Srivastava, N., [9] showed that the present research focuses on developing a continuous one-dimensional model of the metal V-belt CVT in order to understand the influence of pulley flexibility and friction characteristics on its dynamic performance. Friction between the belt and the pulley sheaves was modelled using different mathematical models which account for varying loading scenarios. Simple trigonometric functions were introduced to capture the effects of pulley deformation on the thrust ratio and slip behaviour of the CVT. Modelling the inertial coupling between the belt and the pulley and studying its influence on the dynamic performance of a CVT. The results discuss the influence of friction characteristics and pulley flexibility on the dynamic performance, the axial force requirements, and the torque transmitting capacity of a metal V-belt CVT drive.

Bin Feng [10] showed oil temperature control in a large hydraulic system is dealt with using the fuzzy logic control algorithm. Mathematic model of the control system characterized by large time delay is created based on law of thermodynamics. A self tuning parameter fuzzy PID controller is designed to regulate the cooling water flow rate through the triple proportional valve in order to control the oil temperature. The simulations and experiments are carried out, making a comparison with conventional PID control. It achieved higher control accuracy and temperature, faster response and stronger robustness than conventional PID control system.

Carbone, G., et al [11] dealt with the theoretical and experimental evaluation of the performance of a continuously variable transmission chain drive in steady-state conditions. They proposed an enhanced version of the Carbone–Mangialardi–Mantriota (CMM) model, to accurately predict the slip behaviour and the traction performance of the variator. The theoretical results are discussed and critically compared with experimental data. The comparison confirms the validity of the CMM approach in a large range of clamping forces, speed ratios and torque loads.

Wang, Yubin [13] stated about the electronic-continuously variable transmission (E-CVT) propulsion system for full hybrid electric vehicles (HEVs). Firstly, the E-CVT propulsion systems were classified as two main groups, namely the gear E-CVT and the gearless E-CVT. Consequently, the development of E-CVT propulsion systems is discussed, with emphasis on their system architecture, principle of operation, merits and drawbacks. The Geared E-CVT was found to be more suitable and robust to our application as compared to the gearless setup

Shubham Upadhyaya [14] was written to help you understand this technology and its potential by explaining the operation principle and introducing a simple standard for electric transmission machines' specifications. In this paper, a continuously variable electronic transmission (E-CVT) drive system for a full hybrid was presented. Therefore, the E-CVT drive system's development was discussed focusing on the system architecture, functional principles, and advantages and disadvantages.

Ruan J [15]. Special-designed multi-speed pure electric vehicle–powertrains have been compared and investigated for these applications in this article. Through the optimizing of multiple gear ratios and creating special shifting strategies, a more diverse range of functional needs is realized without increasing the practical size of the electric motor and battery. This article investigated the performance improvements of pure electric vehicle realized through utilization of multi-speed dual-clutch transmissions and continuously variable transmissions. Simulation resulted shows that continuously variable transmission and two-speed transmission are the two most promising transmissions for pure electric vehicle in different classes, respectively.

## **CHAPTER 3**

### **DESIGN OF CVT PARAMETERS**

CVT parameters are designed and selected based on the type of the vehicle, weight of the vehicle, the conditions in which the vehicle will be operated and performance requirements of the CVT etc.

Various CVT parameters are:

1. Centre to centre distance
2. Overall shift ratio
3. Belt type
4. Sheave Dimensions

#### **3.1 CENTER TO CENTER DISTANCE**

It is the distance between the rotation axis of the primary and secondary sheaves. The centre distance has been kept as 8.5 inches for our CVT considering the following factors:

- The C-C distance was finalised according to the requirement of team DJS Kronos India, which participates in BAJA every year. The layout of the vehicle and rulebook is referred by the team for finalising this value
- Length of OEM belts available in the market

#### **3.2 OVERALL SHIFT RATIO**

This was also finalised based on the requirements of the team DJS Kronos India based on the acceleration and top speed desired by the vehicle. The lowest and highest value of ratio of CVT was kept at 0.85 and 3.9 respectively. This led to an overall shift ratio of 4.58.

#### **3.3 BELT TYPE**

Cogged V-belt is used with a wedge angle of 28 degrees. This kind of belt is used as compared to normal straight belt as V-belt allows continuous variable diameters which is important for our CVT performance. These are the dimensions of the selected belt:

- The belt length along the theoretical pitch line is 837.5mm
- Max Width (W) = 22.2mm
- Height (H) = 13.61mm
- Height of Pitch line ( $H_p$ )  $\approx$  6mm

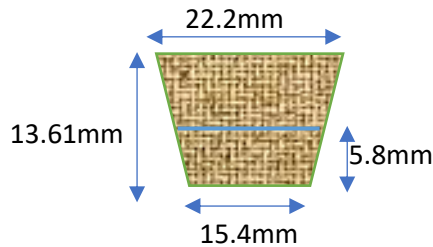


Figure 3.1: CVT belt dimensions

### 3.4 SHEAVE DIMENSIONS

Sheave angle of 14 degrees was finalised due to following factors:

- Availability of stock belts since the sheave angle and belt angle have to approximately equal for efficient performance of the cvt.
- Its effect on the relation between friction and shifting force generated due to the applied axial force
- Generally, a sheave angle of 14 degrees is used in Baja ATVs
- Dimension calculations of the following are shown below:
  - a. Diameters of Primary and secondary sheaves
  - b. Axial Displacement of primary and secondary movable sheaves

#### 3.4.1 DIAMETERS OF PRIMARY AND SECONDARY SHEAVES

Relation between pitch diameters and cvt ratio (From vb bandhari):

$$L = \pi*(D+d)/2 + \beta*(D-d) + 2*C*\cos(\beta)$$

Here,

$$L = 837.5\text{mm}$$

$$B = \sin^{-1}[(D-d)/(2*C)] \quad \& \quad \cos(\beta) = 1 - (D-d)^2/(8*C^2)$$

$$C = 8.5'' = 215.9\text{mm}$$

$$0.85 < R < 3.9$$

Substituting the values, we get

$$837.5 = \pi*(R+1)*d/2 + \sin^{-1}((R-1)*d/(2*215.9))*(R-1)*d + 2*215.9*(1 - ((R-1)*d/2*215.9))^2/2$$

**Putting R=3.9** we get,

$$837.5 = \pi * (3.9+1) * d / 2 + \sin^{-1}((3.9-1) * d / (2 * 215.9)) * (3.9-1) * d + 2 * 215.9 * (1 - ((3.9-1) * d / 2 * 215.9))^2 / 2$$

Solving the above equation we get,

$$d_{\max} = 49.5 \text{ mm}$$

$$D_{\min} = 193 \text{ mm}$$

Therefore,

$$\text{Maximum Inner diameter of primary sheave} = d - 2 * H_p = 49.5 - 2 * 5.8 = 37.9 \text{ mm} \approx 1.5"$$

$$\begin{aligned} \text{Minimum Outer diameter of secondary sheaves} &= D + 2 * (H - H_p) = 193 + 2 * (10.6 - 5.8) \\ &= 205.6 \text{ mm} \approx 8" \end{aligned}$$

**Putting R=0.9** we get,

$$837.5 = \pi * (0.9+1) * d / 2 + \sin^{-1}((0.9-1) * d / (2 * 215.9)) * (0.9-1) * d + 2 * 215.9 * (1 - ((0.9-1) * d / 2 * 215.9))^2 / 2$$

Solving the above equation we get,

$$d_{\min} = 135.9 \text{ mm} \&$$

$$D_{\max} = 122.28 \text{ mm}$$

Therefore

$$\begin{aligned} \text{Minimum Outer diameter of primary sheave} &= d + 2 * (H - H_p) = 135.9 + 2 * (10.6 - 5.8) \\ &= 148.5 \text{ mm} \approx 6" \end{aligned}$$

$$\begin{aligned} \text{Maximum inner diameter of secondary sheaves} &= D - 2 * H_p = 122.3 - 2 * (5.8) \\ &= 110.68 \text{ mm} \approx 4.3" \end{aligned}$$

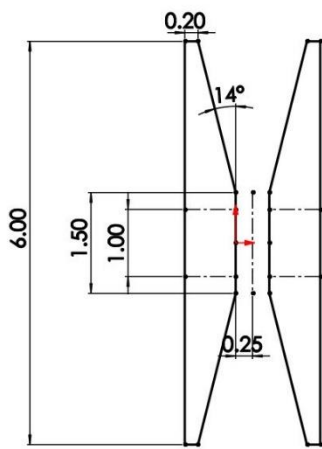


Figure 3.2: Primary Sheave dimensions

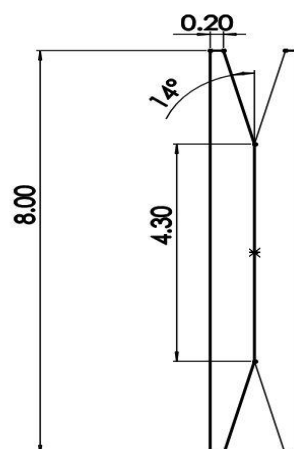


Figure 3.3: Secondary Sheave dimensions

### 3.4.2 AXIAL DISPLACEMENT OF PRIMARY AND SECONDARY MOVABLE SHEAVES

For primary movable sheave,

$$\text{Axial travel} = 2 * (\text{radial travel of belt}) * \tan(\text{sheave angle})$$

$$= (d_{\min} - d_{\max}) * \tan(\text{sheave angle})$$

$$\therefore \text{Axial travel} = (135.9 - 49.5) * \tan(14^\circ) = 21.54 \text{ mm}$$

$$\therefore \text{Total Axial travel} = \text{Axial travel} + \text{Disengaged travel (5mm)}$$

$$= 26.54 \text{ mm} = 1.04"$$

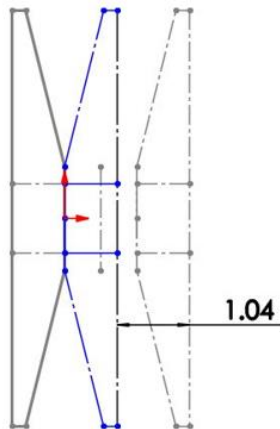


Figure 3.4: Axial displacement of primary movable sheave

For secondary movable sheave,

$$\text{Axial travel} = 2 * (\text{radial travel of belt}) * \tan(\text{sheave angle})$$

$$= (D_{\max} - D_{\min}) * \tan(\text{sheave angle})$$

$$= (193 - 122.28) * \tan(14^\circ) = 17.63 \text{ mm} = 0.69"$$

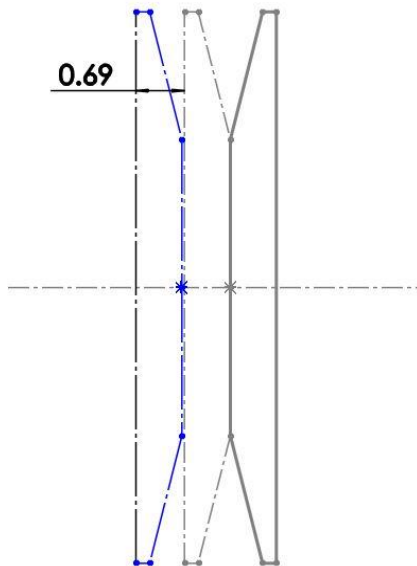


Figure 3.5: Axial displacement of secondary movable sheave

## **CHAPTER 4**

### **METHODOLOGY FOR MATERIAL SELECTION**

#### **4.1 OBJECTIVES**

To design and analyse the problems being faced in an ATV and overcome all those flaws. Major flaws include weight, size, and cost. Occasional breakdowns and maintenance have been observed. Design plan includes research and material selection for the sheaves, motor mounts, fork, bearing Housings, and power screws and Nut. The material is selected based on factors such as strength, weight, cost, and availability. Ansys software is used along with manual calculations to ensure reliability of design. Standard dimensions like the minimum dimensions are selected and modelled in a CAD software.

#### **4.2 DESIGN SELECTION & MATERIAL SELECTION CRITERIA**

The primary and secondary sheaves of the CVT transmits the torque of the engine to the gearbox. Since it has the highest rpm, losses associated with them are also higher. Hence it is important to select a material which can offer sufficient wear resistance as well as minimum load to increase the overall efficiency of the vehicle.

The bearing housings will be made from mild steel because stress generated on these components are less and they are only needed to restrict the bearing on the shaft assembly. Along with that, mild steel is easily available and cheap to procure and machine.

Motor mounts are used to mount the stepper motor to the engine or gearbox of the ATV and experiences very high forces. The output shaft of these motors is connected to power screws. It will in-turn be connected to the sheaves and will provide the force required to move the sheaves of primary and secondary CVT along the rotating axis depending on the required gear reduction. Possible options were aluminium alloy (7000 series) or steel alloys (En series). Here steel alloys were considered due to cost limitations and due to deflection criteria. Also, since the mount is not a rotating component, losses associated with it are also small and hence selecting an expensive material (al-alloy) will not be cost effective.

Fork is what transmits the axial motion from stepper motor to the primary and secondary sheaves. One end of the fork is connected to the nut of power screws, and the other end is hinged on the bearing housing which is fixed. Since the fork is used to transmit force, it experiences highest level of stresses and deformation. Hence En series of alloy steel is used for fork material.

The fork and the sheaves are in contact with each other via a roller wheel to avoid relative motion, since one component (fork) is non-rotating, and the sheave is rotating. The wheel is machined using brass since it has properties such as wear resistance, easy machinability etc.

which are favourable for this application as the roller wheel is supposed to pure roll on the sheaves.

Other miscellaneous parts such as fork fillers, spacers etc. are machined using mild steel or aluminium alloy depending on the load and motion it experiences.

The gearbox casing which is used to mount the motor mount is fabricated using aluminium 6061-T6. The consideration involved in the selection of material for the gearbox is done by Team DJS Kronos India taking onto account the forces acted upon it due to torque transmission, forces on mounting points, impact forces, fatigue life etc.

<b>Material</b>	<b>Yield Strength (MPa)</b>	<b>Density (Kg/m<sup>3</sup>)</b>	<b>Cost (Per Kg) in Rs</b>
EN24 Steel	550	7850	110
EN8 Steel	415	7850	105
AISI 9310 Steel	690	7850	120
Cast Iron	350	7150	80
Al-6061	280	2700	300
Al-7075	540	2700	650
Mild Steel	250	7850	80

Table 4.1: Characteristics of various materials

The above table was referenced while selecting the material for each component. Factors such as strength, weight and cost were considered and the final material was finalised using a selection matrix.

<b>Part</b>	<b>Material used</b>	<b>FOS</b>
Motor Mount 1 & 2	En-24	2-2.5
Primary Fork	En-24	2
Bearing Housings	Mild Steel	3
Roller wheels	Brass	2

Power screw components	Hardened steel (OEM)	-
Primary & Secondary Sheaves	Al-6061 T6	2-2.5
Motor Adaptor	Hardened Steel (OEM)	-
Miscellaneous items	Mild Steel	-

Table 4.2: Material selected for various components

### 4.3 SELECTION OF FITS AND TOLERANCES

Hole basis system is used for the fit between the inner race of bearing and the shaft since the bearing bearings comes in standard sizes. Hence, the shaft should be manufactured accordingly.

For the fit between the outer race of the bearing and the casing, the outer race has a fixed dimension. Hence, we shaft basis is followed and the hole is machined accordingly. A clearance fit between the mating components will result in too much sliding and an interference fit would result in extra stresses on the mating parts. From the legacy data we have, a tight interference fit between the inner race of bearing and the shaft resulted in radial pressure on the ball bearings which resulted in the failure of the bearing. Hence, a transition fit with a tolerance grade based on previous research is decided. Hole basis system and shaft basis system used is referred from V.B. Bhandari design data book.

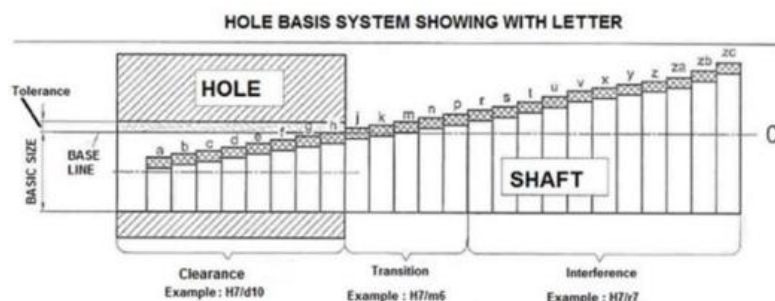


Figure 4.1: Hole basis system

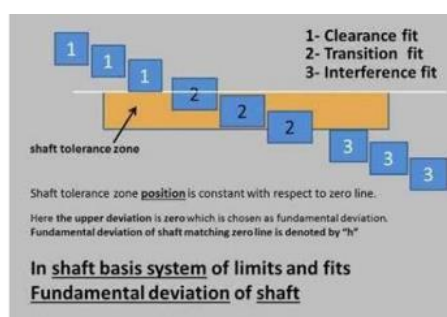


Figure 4.2: Shaft basis system

## **CHAPTER 5**

### **DESIGN & ANALYSIS OF CVT ACTUATION MECHANISM**

Before mechanism for the axial motion of the primary and secondary sheaves it is important to know the maximum axial force required during shifting of sheaves. Based on the legacy data:

Maximum Axial Force for Primary = 4kN

Maximum Axial Force for Secondary = 3kN

Hence, the motor selected can provide a force of over 4.5kN

#### **5.1 PRIMARY CVT ACTUATION MECHANISM**

The sheave to actuate in primary side of CVT is away from the engine and requires higher force than secondary. Considering different mounting options, engine block was the best option. Hence, a fork lever mechanism hinged over the engine output/CVT input shaft is designed to achieve a mechanical advantage.

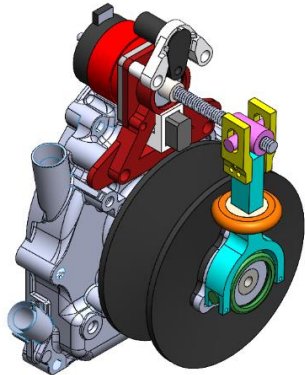


Figure 5.1: E-CVT Primary Sheave Assembly

The primary sheave assembly has the following components:

- Stepper Motor
- Motor Mount (Red)
- Adapter
- Power Screw
- Nut (Pink)
- Slotted Link (Yellow)
- Hinged Fork (Blue)
- Pivot and Bearing Housing (Green)
- Roller (Orange)
- Roller's Bearing
- Optical RPM and Hall Sensors Mount

The motor mount is fixed on the engine block aligning the motor with enough clearances. An adapter connects the motor shaft and power screw rigidly. Nut translates on the power screw limited by a jam nut. The rectangular cross section of nut limits rotation. The fork assembly is supported by the pivot and bearing housing on the CVT input shaft. The Roller and roller bearing are press fitted on the fork. A detachable slotted link connects fork and sliding nut.

For high force, mechanical advantage happens in two stages. First at the trapezoidal lead screw and second at the hinged fork. A processing unit signals the stepper motor to rotate by a certain angle. This in turn rotates the power screw and the nut translates, applying a force at the end of the fork lever. A moment is transmitted by the fork to the roller. The roller is in point contact with the movable sheave and can rotate freely. Small contact area and free rotation eliminates any heating issues. The force is transmitted successfully to sheave and translate over the guide on shaft. Hence the rotational motion of motor is successfully transmitted into translation motion of sheave.

The power screw pitch and the distance of roller from the pivot can be changed for application in other vehicles with different force requirements or low motor power space. This assembly can also be used for modifying gagged CVT and convert them into an E-CVT.

### 5.1.1 DESIGN OF LEAD SCREW AND NUT:

A M8 single start lead screw with 1mm pitch has been selected for our requirements. A 1mm per revolution lead is provided by this pair of nut and bolt. High axial force requirement of the movable primary sheave is kept in mind while selection. The operating speed is low, so the friction should not result in significant efficiency loss.

Torque and axial force relation:

Since Rotational Input = Linear Output Power

$$\therefore \text{Torque} * \text{RPM} * \frac{2\pi}{60} = F_{\text{axial}} * \frac{\text{Distance between pivot & Nut}}{\text{Distance between pivot & roller}} * \text{velocity}$$

$$\text{Also, } \text{velocity} = \frac{\text{RPM}}{60000}$$

$$\therefore \text{Torque} * \text{RPM} * \frac{2\pi}{60} = F_{\text{axial}} * \frac{\text{Distance between pivot & Nut}}{\text{Distance between pivot & roller}} * \frac{\text{RPM}}{60000}$$

$$\therefore \text{Torque} = 0.28 \text{ N-m}$$

Using this torque as the reference the motor was selected with suitable power, RPM, and torque ratings.

Length of lead screw:

$$L_{\text{screw}} = \frac{\text{Adaptor Length}}{2} + \text{Sheave Travel} + \text{Threaded Nut Length} \\ + \text{Fixed Sheave Width}$$

Here, Threaded nut length = 30 mm (OEM Length)

Sheave Travel = 26.54 mm (Calculated earlier)

Adaptor Length = 20 mm (OEM length)

Fixed Sheave Width = 15.7 mm

$$\therefore L_{screw} = 10 + 26.54 + 30 + 15.7$$

$$\therefore L_{screw} = 82.24 \text{ mm}$$

Selection of roller bearing:

A roller bearing is used to support roller pulling movable sheave of primary CVT.

Force acting on roller wheel = 4500 N

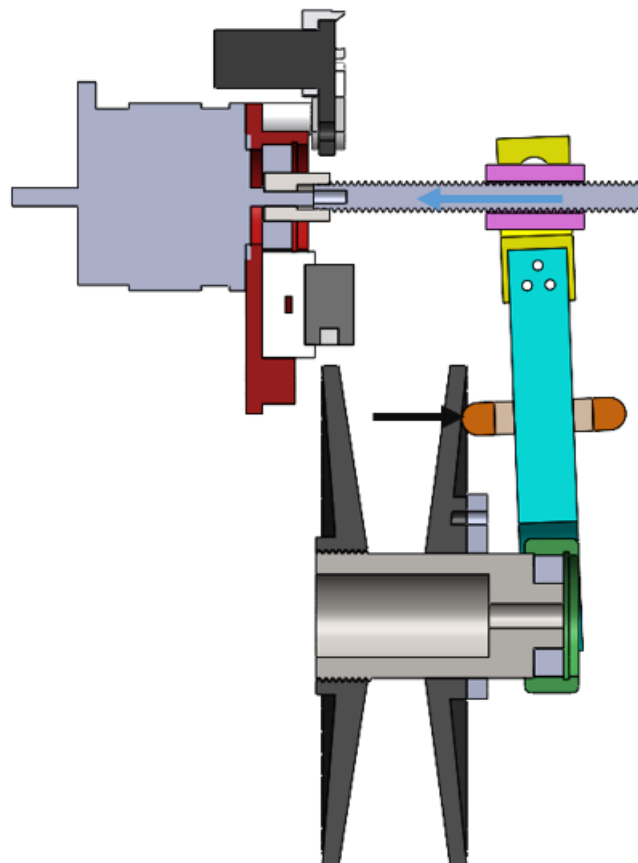


Figure 5.2: Force visualization of Primary Sheave Assembly

$$\text{Using, } L_{10} = \left(\frac{C}{P}\right)^k$$

$$\text{Here, } L_{10} = \text{Life in Million Revolutions} = RPM * 60 * \frac{\text{Life in hours}}{10^6}$$

$$= 350 * 60 * \frac{60}{10^6} \text{ (Life in hours is assumed to be 60 hrs)}$$

$$= 1.26$$

$C$  = Dynamic Capacity of Bearing

$$P = \text{Equivalent Load} = \text{Force} * C_s * k_t = 4500 * 1.2 * 1 = 4800 \text{ N}$$

$K$  = 3 (For Ball Bearing)

Substituting the above values we get,

$$1.26 = \left( \frac{C}{4800} \right)^3$$

$$\therefore C = 5184 \text{ N}$$

Selecting 6200-2Z bearing from the SKF catalogue with,

Dynamic capacity = 5400 N,

$b = 10 \text{ mm}$

$Width = 9 \text{ mm}$

### 5.1.2 DESIGN & ANALYSIS OF MOTOR MOUNT:

Initially keeping in mind, the movable sheave, we tried to position the motor on chassis and have a simpler mechanism and assembly. But large alignment issues can arise in a scenario of deformation of chassis by any type of impact. So, engine block was finalized for mounting motor, eliminating concentricity alignment issues.

1<sup>st</sup> iteration:

Designed the stepper motor mount with considerations of clearances and out of sheet metal for ease in manufacturing.



Figure 5.3: Primary Motor mount iteration 1  
Stress analysis revealed failure of the part with given loading conditions

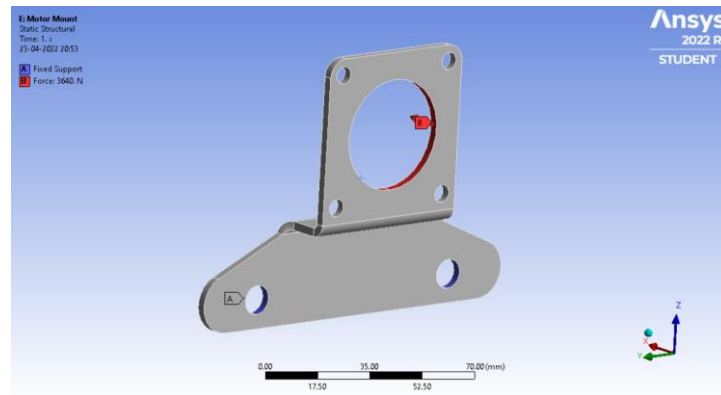


Figure 5.4: Primary Motor mount iteration 1 loading condition

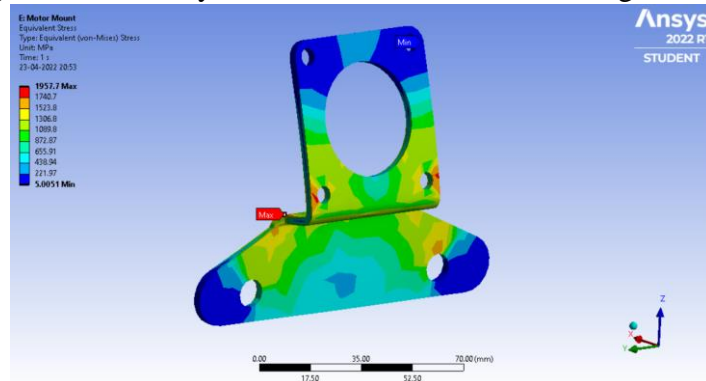


Figure 5.5: Primary Motor mount iteration 1 analysis

## 2<sup>nd</sup> Iteration:

Designed the mount for increased strength made from machined metal block.

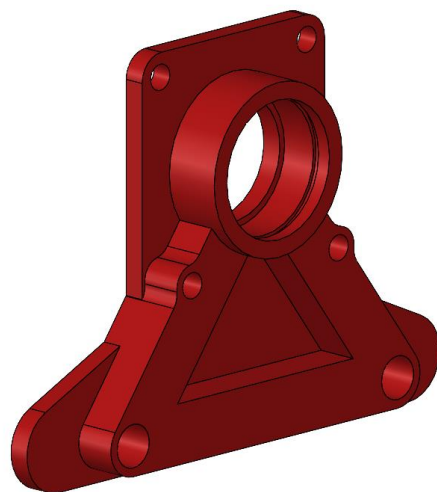


Figure 5.6: Primary Motor mount iteration 2

The result of stress analysis of the 2<sup>nd</sup> iteration is:

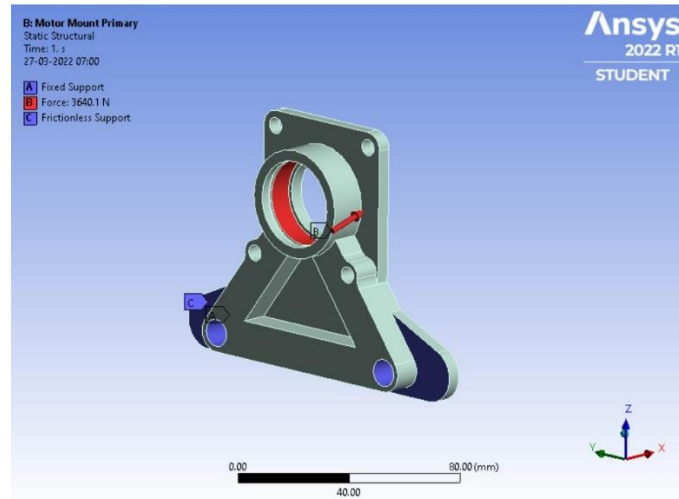


Figure 5.7: Primary Motor mount iteration 2 loading condition

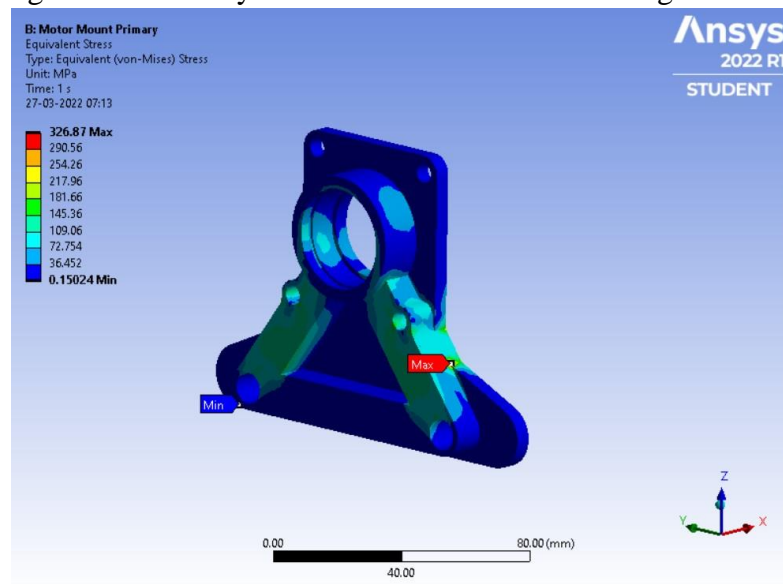


Figure 5.8: Primary Motor mount iteration 2 analysis

It had an FOS of 2.08 and hence the design was finalised.

### 5.1.3 DESIGN & ANALYSIS OF FORK & NUT ASSEMBLY:

#### 1<sup>st</sup> Iteration:

The following design was made for conceptualization.

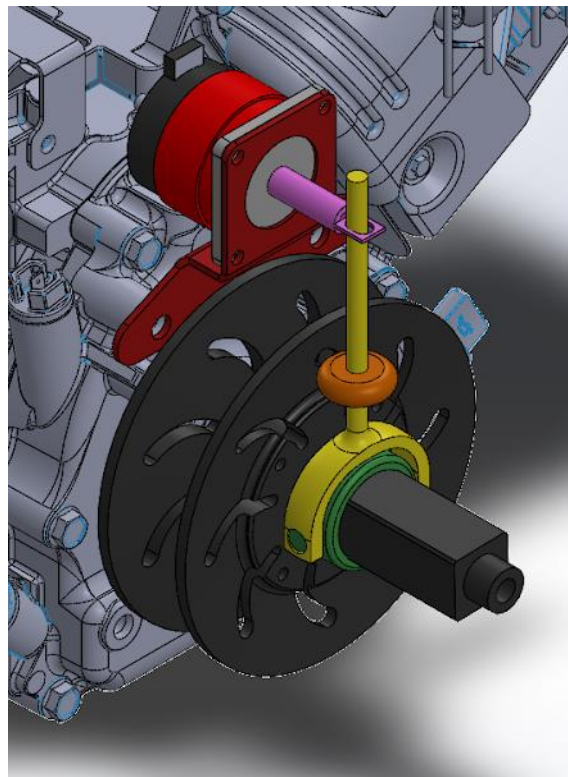


Figure 5.9: Fork and Nut assembly iteration 1

#### 2<sup>nd</sup> Iteration:

This design was made after considering a design for assembly and strength required. Slotted guide was shifted to the fork from nut and the fork Slotted end was split into three parts for assembly. Pivoting end of fork is slotted for easily sliding into “Pivot and Bearing Housing” and then restricted with a M3 Bolt.

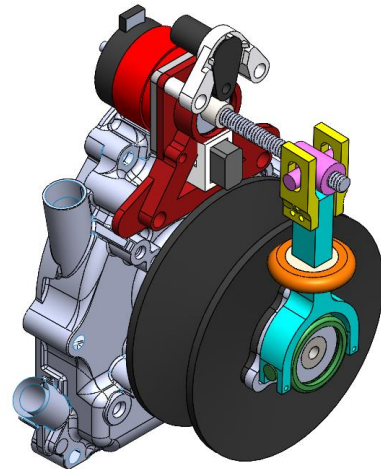


Figure 5.10: Fork and Nut assembly iteration 2

### Stress Analysis Results:

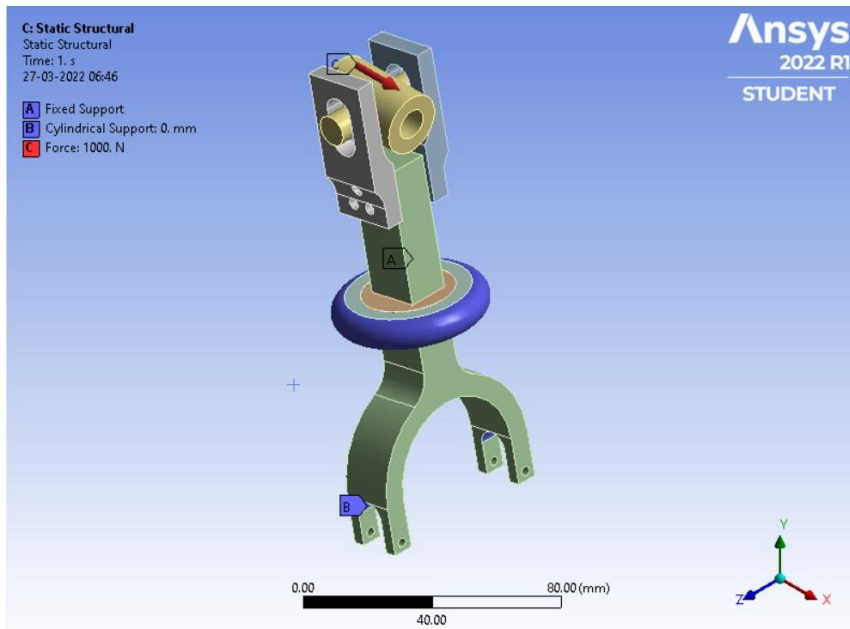


Figure 5.11: Fork and Nut assembly iteration 2 loading condition

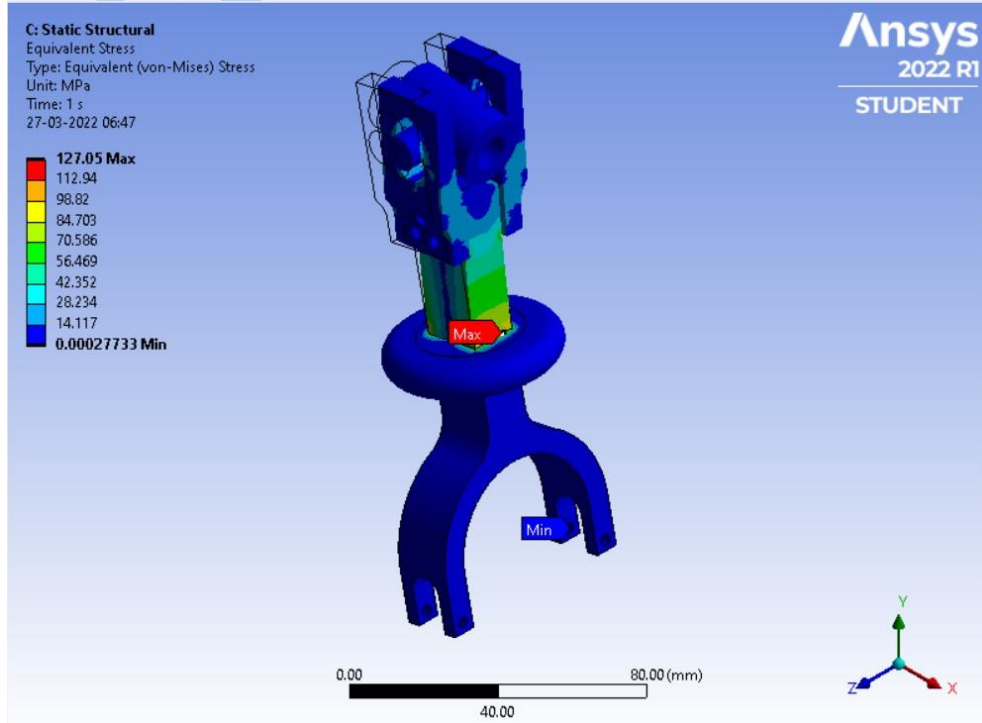


Figure 5.12: Fork and Nut assembly iteration 2 analysis

This iteration had a FOS of 2 and the design was finalized

#### 5.1.4 DESIGN & ANALYSIS OF PRIMARY CVT:

For the design analysis of the Primary CVT, Failure due to torsion was considered. The input torque of 76.44 N-m which is equal to the engine torque is taken.



Figure 5.13: Exploded view of primary CVT

##### 1. Shaft of Primary CVT:

This component is responsible for transferring torque from the engine to the input shaft of the CVT. The material for this component is hardened En-24 as this component experiences relative motion with respect to the keyway adaptor due to the axial motion of the movable sheave.

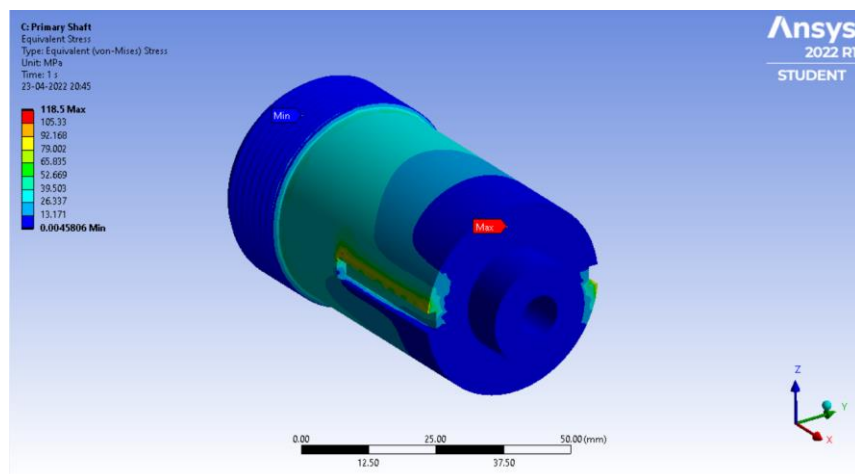


Figure 5.14: Shaft of primary CVT analysis

## 2. Keyway Adaptor:

As the primary CVT's aluminium movable sheaves is supposed to slide on the secondary CVT shaft, which is hardened steel, an attachment with keyway slots will be bolted to the movable sheaves. This component is responsible for transfer of torque from movable sheave to the secondary CVT shaft. This component will not be hardened.

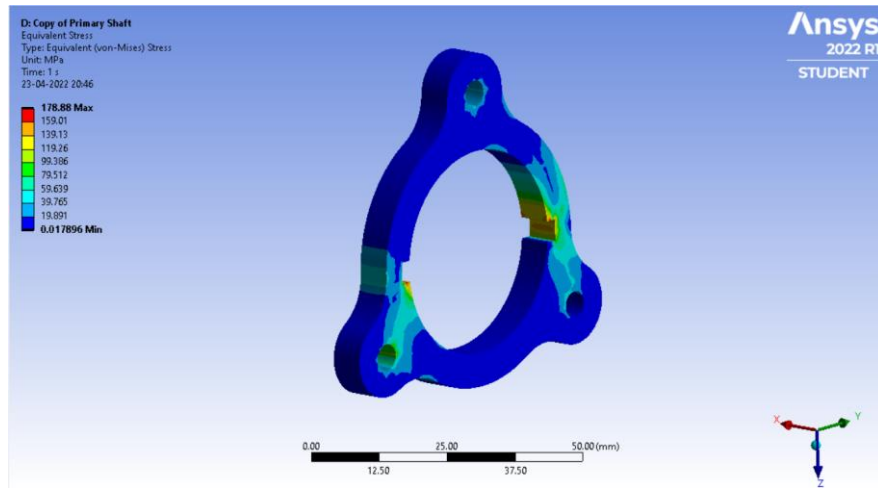


Figure 5.15: Keyway adaptor of primary CVT analysis

## 3. Primary Sheaves:

The sheaves transmit engine power to the belt via friction. This frictional force is acted upon the angle called angle of wrap which varies according to the CVT ratio. For analysis purposes the worst situation with minimum angle of wrap is considered with maximum torque transfer taking place.

Fixed Sheave:

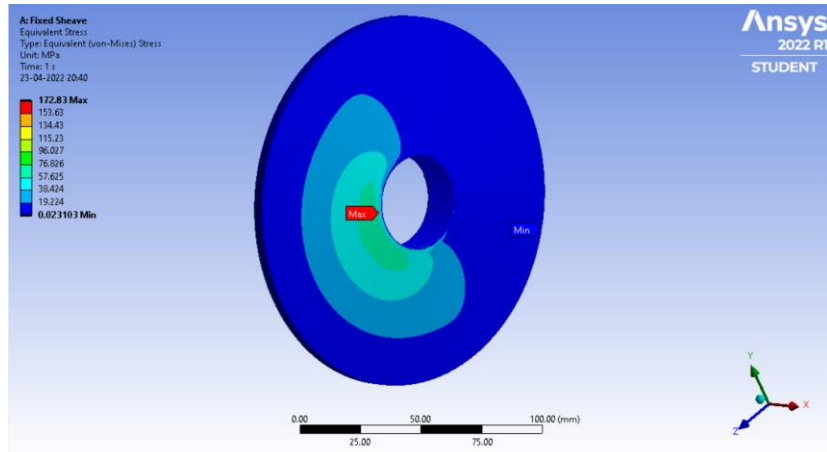


Figure 5.16: Fixed sheave of primary CVT analysis

Movable Sheave:

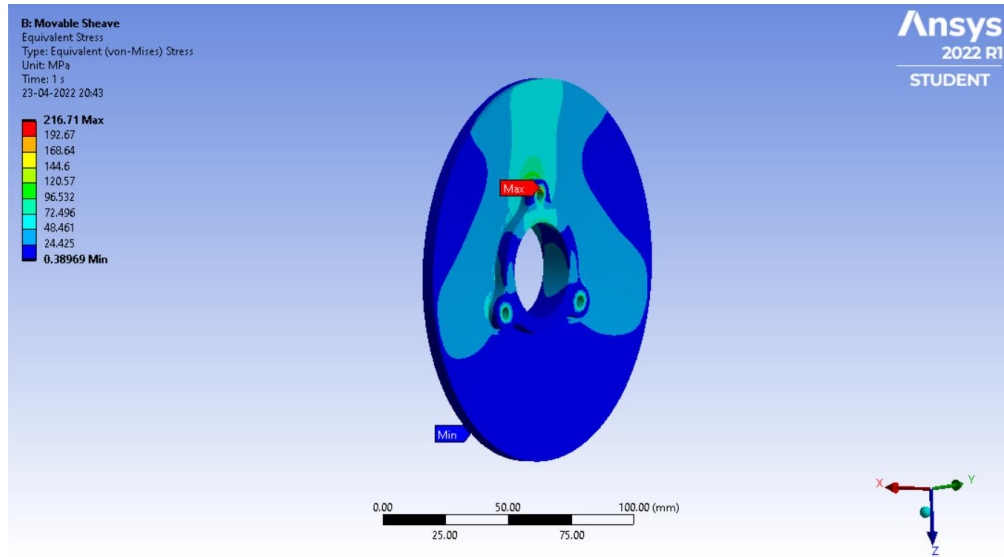


Figure 5.17: Movable sheave of primary CVT analysis

## 5.2 SECONDARY CVT ACTUATION MECHANISM

Since the force required by secondary sheave is well below the motor limit, the sheaves will be actuated directly by connecting the output of power screw to the sheaves as compared to primary mechanism where the force required is high and a hinged mechanism is used for mechanical advantage.

### Working:

The selected stepper motor will be mounted on the gearbox of the ATV for rigid support. The output of the stepper motor will be connected to the trapezoidal screw and nut arrangement via a motor adaptor. The motor mount will also house the bearing to support the motor shaft to avoid any sudden reaction load from the secondary sheaves to motor axle and cause damage. The nut will have two rollers mounted on it to avoid relative motion between the stationary nut and rotating sheave surface. These roller mounts and the nut will be integrated into a component called ‘Integrated Nut’. The integrated nut will push the movable sheave of the secondary CVT to required position at the required moment. The rotation of the integrated nut must be restricted and hence a support is designed that restricts the rotation of integrated nut about the motor axle and permits linear motion along the axle length. The length of the Screw was calculated using the sheave travel length, Adapter length, Nut length etc.

### 5.2.1 DESIGN OF LEAD SCREW & NUT

A M8 single start lead screw with 1mm pitch has been selected for our requirements. This set of screw and nut arrangement will have a lead of 1mm per revolution. The selection was made keeping in mind the high axial force required for the axial movement of the

secondary movable sheaves. Although efficiency loss due to friction is high in the screws and nuts of the selected specification, it won't hinder us much as the working speed is not high.

#### Torque and axial force relation:

Since Rotational Input power = Linear Output power

$$\therefore \text{Torque} * \text{RPM} * 2\pi / 60 = F_{\text{axial}} * \text{velocity}$$

Also, Velocity = (RPM/60,000)

$$\therefore \text{Torque} * \text{RPM} * 2\pi / 60 = F_{\text{axial}} * \text{RPM} / 60,000$$

$$\therefore \text{Torque} = 0.64 \text{ N-m}$$

Using this torque as the reference the motor was selected with suitable rpm.

#### Length of Lead screw:

$$L_{\text{screw}} = (\text{Adaptor Length})/2 + \text{Sheave travel} + \text{Threaded Nut length}$$

Here, Threaded nut length = 15mm (OEM length)

Sheave travel = 17.5mm (calculated earlier)

Adaptor length = 20 mm (OEM length)

$$\therefore L_{\text{screw}} = 10 + 17.5 + 15$$

$$= 42.5 \text{ mm}$$

#### Selection of Roller Bearings:

Since 2 rollers are used to push the movable sheave of the secondary CVT, the force applied by the trapezoidal nut of the lead screw is transmitted through the brass roller wheels. The distribution of force is assumed to be equal among the two roller wheels.

$$\therefore \text{Force acting on each roller wheel} = 4000/2 = 2000 \text{ N.}$$

Using,  $L_{10} = (C/P)^k$

$$\text{Here, } L_{10} = \text{Life in Mrevs} = \text{RPM} * 60 * (\text{Life in hours}) / 10^6$$

$$= 350 * 60 * 60 / 10^6 \quad (\text{Life in hours is assumed to be 60 hrs})$$

$$= 1.26$$

C = Dynamic Capacity of bearing

$$P = \text{Equivalent load} = \text{Force} * C_s * k_t = 4000 * 1.2 * 1 = 4800 \text{ N}$$

K = 3 for ball bearings.

Substituting the above values we get,

$$1.26 = (C/4800)^3$$

$$\therefore C = 5184 \text{ N}$$

Selecting 6200-2Z bearing from the SKF catalogue with dynamic capacity of 5400N, b=10mm, D= 30mm and width=9mm

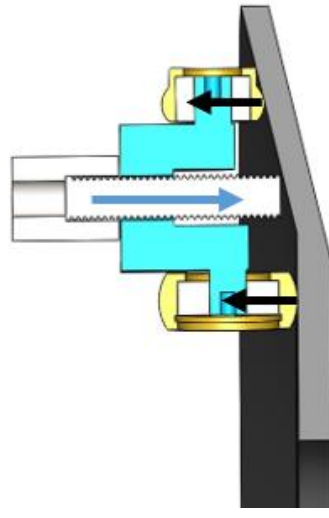


Figure 5.18: Force visualisation of integrated nut assembly

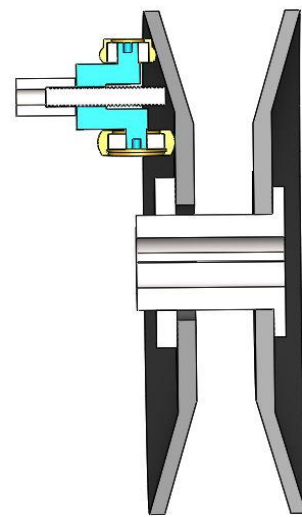


Figure 5.19: Sectional view of secondary sheave assembly

### 5.2.2 DESIGN & ANALYSIS OF MOTOR MOUNT

The concept design of motor mount was done using the layout of the vehicle and clearance of the mount and stepper motor from the engine and other components of the vehicle.

1<sup>st</sup> design of stepper motor mount taking only clearances into consideration

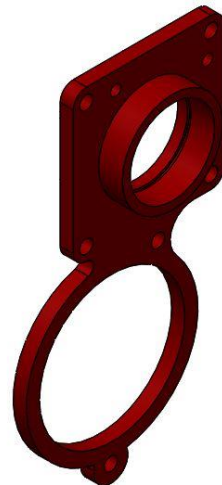


Figure 5.20: Secondary motor mount iteration 1

### Stress Analysis:

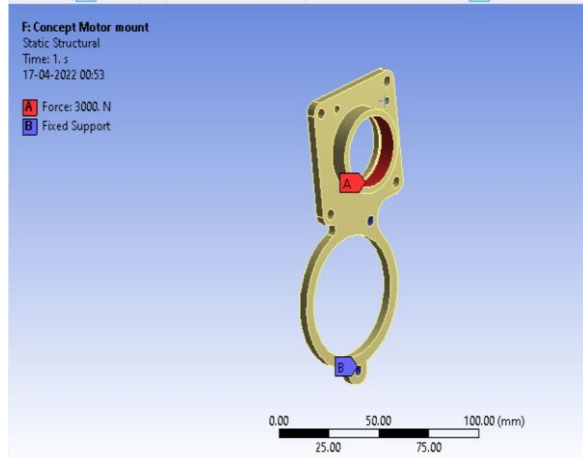


Figure 5.21: Secondary motor mount iteration 1 loading condition

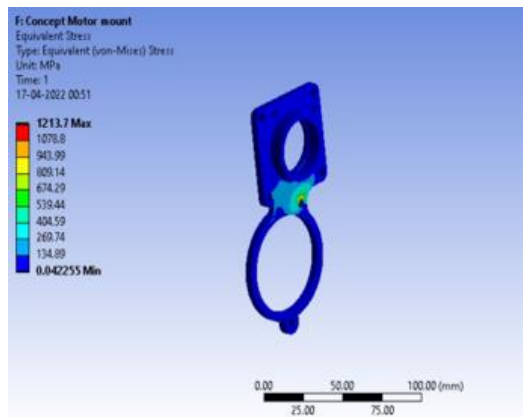


Figure 5.22: Secondary motor mount iteration 1 analysis

The motor mount design was further strengthened and redesigned



Figure 5.23: Secondary motor mount iteration 2

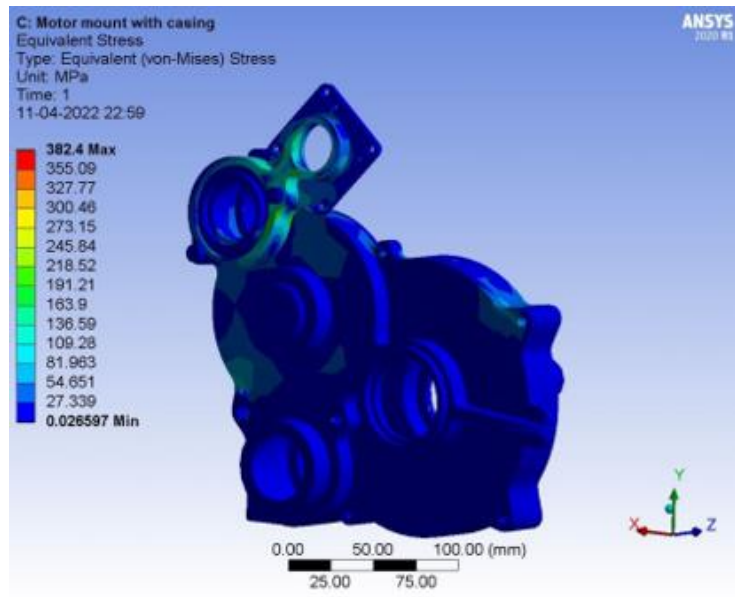


Figure 5.24: Secondary motor mount iteration 2 analysis

### 5.2.3 DESIGN & ANALYSIS OF INTEGRATED NUT

The axial force required for shifting is being acted upon the part of internal threading of the integrated nut. The force is split between the 2 rollers and is transmitted to sheaves as shown below.

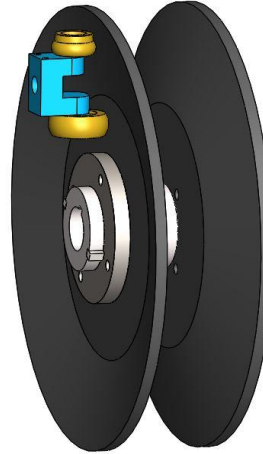


Figure 5.25: Secondary Integrated Nut

### Stress Analysis:

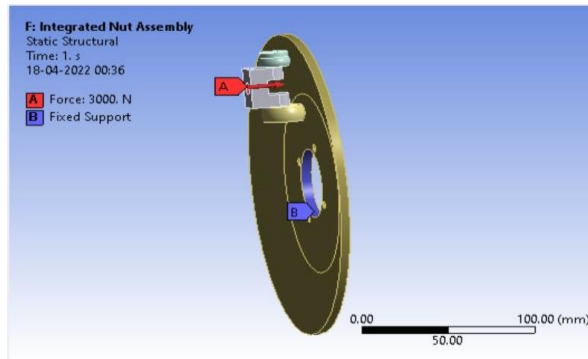


Figure 5.26: Secondary Integrated Nut loading condition

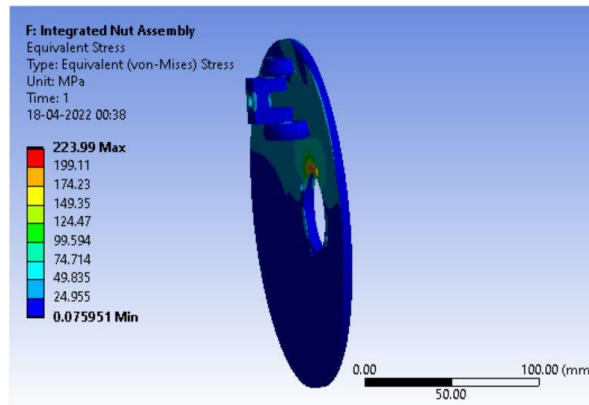


Figure 5.27: Secondary Integrated Nut analysis

### **5.2.3 DESIGN & ANALYSIS OF SECONADARY CVT**

For the design analysis of the secondary CVT torsional failure analysis was carried out. The input torque of 76.44N·m which is equal to the engine torque is taken.

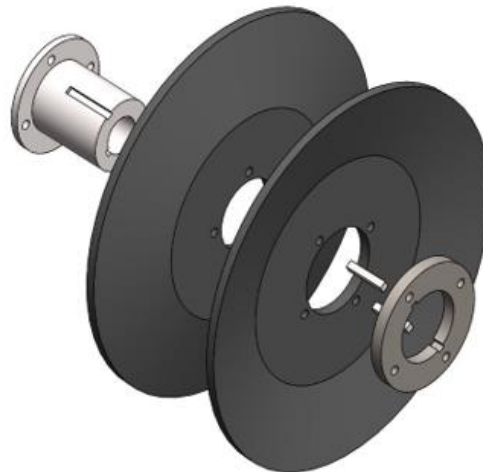


Figure 5.28: Secondary CVT exploded view

## 1. Shaft of Secondary CVT:

This component is responsible for transferring torque from the sheaves of secondary CVT to the input shaft of the gearbox. The material for this component is hardened En-24 as this component experiences relative motion wrt the keyway adaptor due to the axial motion of the movable sheave

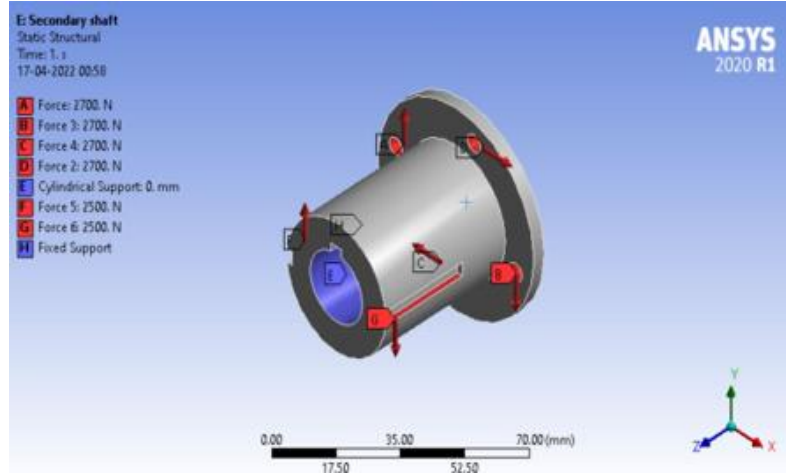


Figure 5.29: Shaft of Secondary CVT loading condition

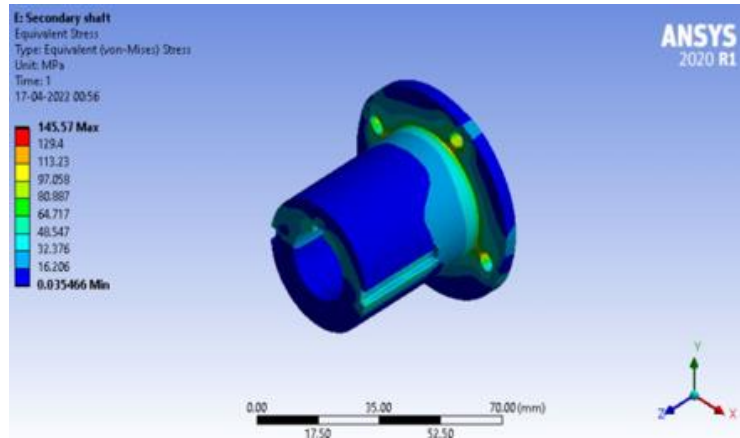


Figure 5.30: Shaft of Secondary CVT analysis

## 2. Keyway Adaptor:

As the secondary CVT's aluminium movable sheaves are supposed to slide on the secondary CVT shaft which is hardened steel, an attachment with keyway slots will be bolted to the movable sheaves. This component is responsible for transfer of torque from movable sheave to the secondary CVT shaft. This component will not be hardened

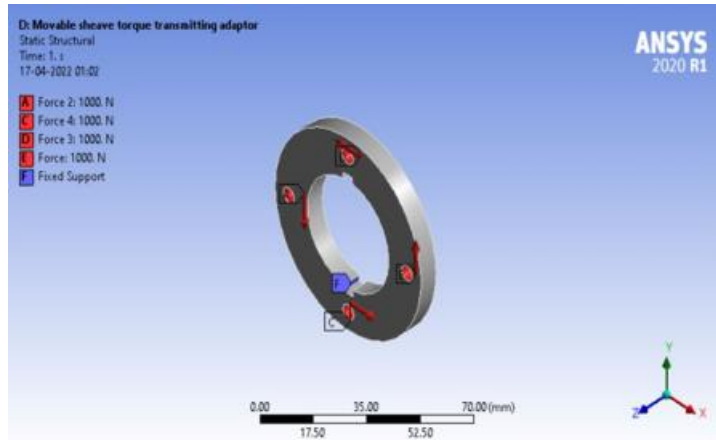


Figure 5.31: Keyway adaptor of Secondary CVT loading condition

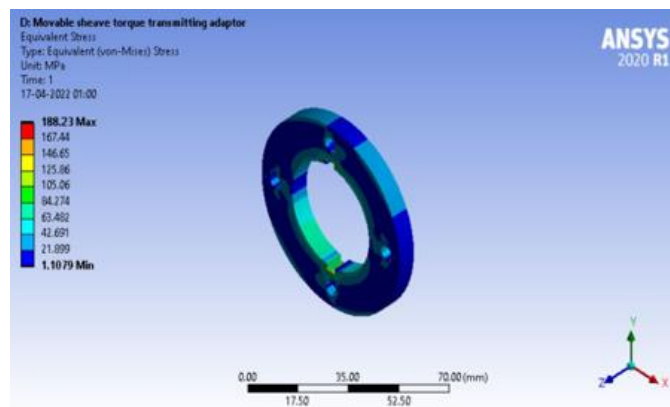


Figure 5.32: Keyway adaptor of Secondary CVT analysis

### 3. Secondary Sheaves:

The belt transmits engine power to the sheaves via friction. This frictional force is acted upon the angle called angle of wrap which varies according to the CVT ratio. For analysis purposes the worst situation with minimum angle of wrap is considered with maximum torque transfer taking place.

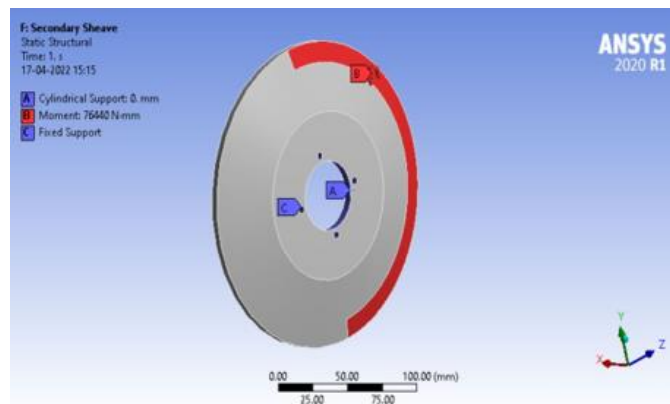


Figure 5.33: Sheaves of Secondary CVT Loading condition

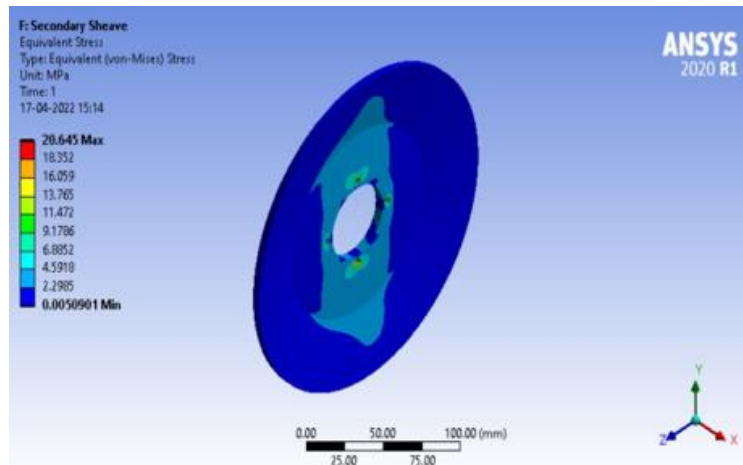


Figure 5.34: Sheaves of Secondary CVT analysis

### 5.3 DESIGN OF SENSOR MOUNTS

#### 1. Optical RPM Sensor:

It mounted near the over the fixed sheave for measuring Primary CVT RPM. While for measuring RPM of Secondary CVT, it is mounted over the gearbox input shaft.

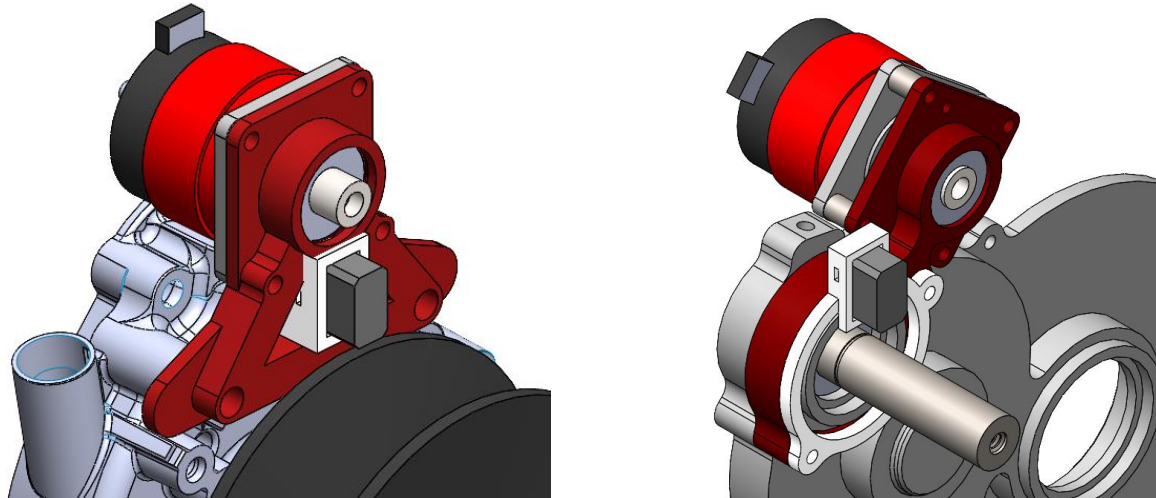


Figure 5.35: Optical RPM sensor mounts on primary and secondary CVT

#### 2. Hall Sensor:

Hall sensor mounts are fixed on two bolting holes of motor mounts and spaced using spacers maintaining clearances.

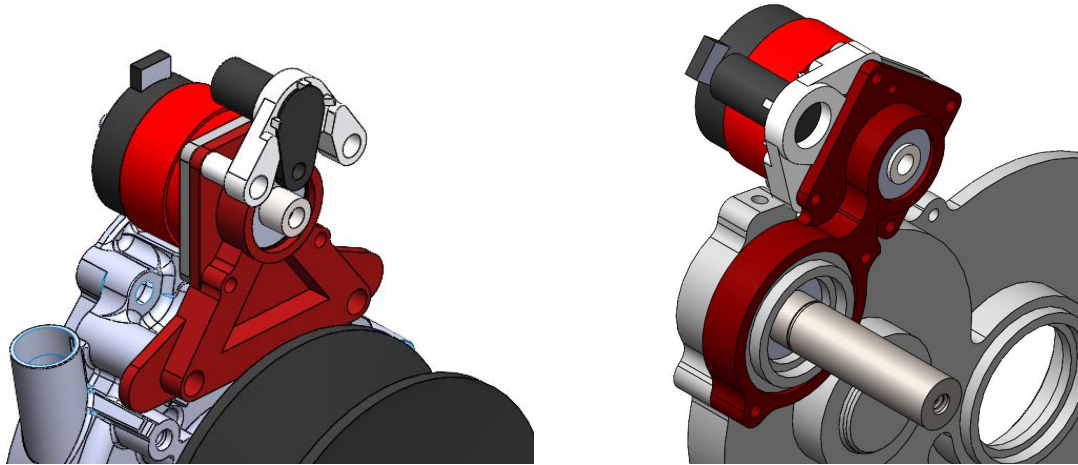


Figure 5.36: Hall sensor mounts on primary and secondary CVT

# CHAPTER 6

## DESIGN & SELECTION OF ELECTRONIC COMPONENTS

### 6.1 MOTOR SELECTION

#### Stepper Motor

A stepper motor is a type of DC brushless motor that has motion divided to small angle steps. The motor steps around by pulsing alternating electromagnetic coils incrementing a gear with teeth attracted to the magnetic coils. Applying a voltage, the motor applies constant holding torque however the strength of this magnetic field is not very controllable. The motor rotates very slowly but very high torque meaning no reduction will likely be needed in our application. Closed loop control is not needed to get reasonably repeatable position control however, it can lose count if a step is missed. The form of the motor is very flat and does not stick out very much past the CVT case.

**Pros:** Steppers have small profiles making packing inside the chassis very simple. The high torque produced by a stepper with no reduction need

**Cons:** Can lose steps easily if max load exceeded. Constant power draw.



Figure 6.1: Stepper Motor

## Brushless DC Motor

A brushless DC motor, BLDC, is powered by DC electricity via an inverter or switching powersupply which produces an AC electric current to drive each phase of the motor via a closed loop controller. The controller provides pulses of current to the motor windings that control the speed and torque of the motor. This motor typically operates at speed in the thousands of rpm meaning a reduction will be needed to operate at the speeds needed for our application.

**Pros:** Very high torque, strong brake force. Smaller in size and packaging. Small time constant.

**Cons:** Expensive, Needs a designated driver circuit.



Figure 6.2: Brushless DC motor

## **Brushed DC Motor**

The brushed DC motor is most simple and widely used motor. Closed loop control can be easily implemented to control position, velocity, or torque. The average operating speed of roughly in the thousands of rpm so a reduction will be required. The brushes in the motor are wear prone and must be replaced. However, the short lifetime of the Baja Car that this may not be a concern. These motors are very long and could lead to issues with fitting in with the current rear packaging of the Baja car.

**Pros:** Simple, inexpensive, versatile. Only power and ground required. Responds to PWM.

**Cons:** Large Form Factor and a gear reduction needed. Brushes cause sparks and wear.



Figure 6.3: Brushed DC Motor

## **Linear Magnetic Actuator**

An electromagnetic actuator takes electricity and converts it into magnetic force. Magnetic force is used to move the spool or poppet which in turn controls the direction of flow. The actuator is very long and will not fit well in the packaging. Due to the complex coil designs needed, the actuators are expensive.

**Pros:** Motion already linear. Open loop control.

**Cons:** Only precise force control. Expensive to purchase. Very long and bad for packaging.



Figure 6.4: Linear Magnetic Actuator

## Motor Selection Matrix

Motor	Packaging	Position Control	Torque Control	Controller Cost	Additional Reduction	Total Score
<b>Brushed DC motor</b>	1	5	5	2	0	13
<b>BLDC</b>	2	5	5	0	0	12
<b>Stepper Motor</b>	<b>3</b>	<b>4</b>	<b>4</b>	<b>2</b>	<b>1</b>	<b>14</b>
<b>Linear Magnetic Actuator</b>	0	2	4	0	3	9

Table 6.1: Motor selection matrix

Based on the above considerations the Stepper motor is the ideal choice for our project as it fulfils all the required parameters and although traditionally Stepper motor has weak torque control but if coupled with a motor driver with electronically controllable current limit, it should also be possible to control the torque with is true in the pololu motor drivers.

## Stepper Motor Selection

### **PM "Permanent Magnet" Type**

This is a stepper motor whose rotor is made from two permanent magnet rotors which are slightly offset from each other. The permanent magnet is axially magnetized; meaning that the north and south poles alternate and are on the same axis as the motor shaft. When current is applied to windings, poles on the stator are magnetized and align with the opposite poles from the permanent magnet rotor. A widely used PM type stepper motor is the 2-phase claw type as shown below

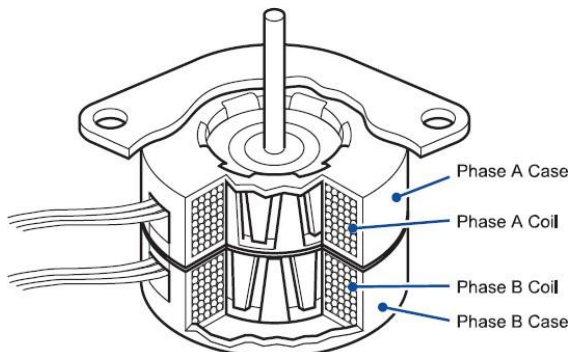


Figure 6.5: Permanent Magnet Stepper Motor

If the number of poles or the number of phases increase, the step angle would decrease. However, as the number of poles increases, the magnetic force and torque also become weaker. A PM type stepper motor is simple in construction and inexpensive to manufacture. The permanent magnets allow PM type stepper motors to output higher torque. However, high speed performance is limited due to large loss during rotation. With micro stepping, the driver's ability to control current precisely at each phase becomes increasingly important in determining the motor's repetitive position accuracy. Another difference is that PM type stepper motors uses constant voltage drivers, which are more difficult to use than constant current chopper drivers.

### **VR "Variable Reluctance" Type**

This is a stepper motor which provides teeth on the rotor and stator where the magnetic forces are concentrated. It offers the simplest design out of the three types discussed here. A VR type stepper motor has no magnets, which means it cannot output holding torque or detent torque at standstill.

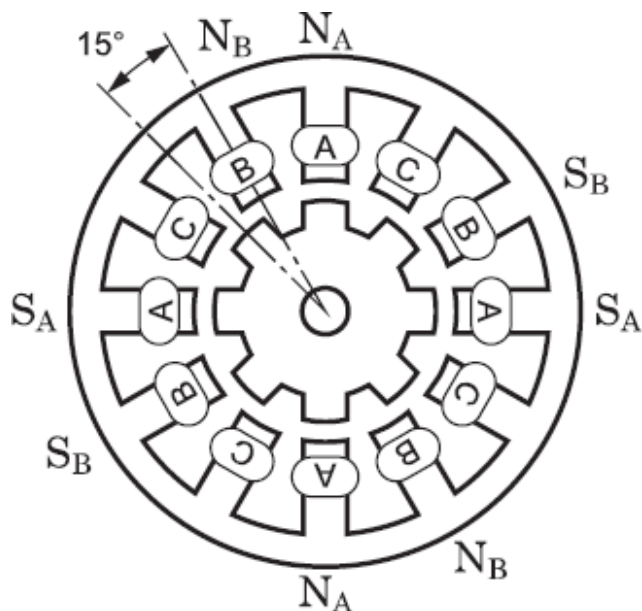


Figure 6.6: Variable Reluctance Stepper Motor

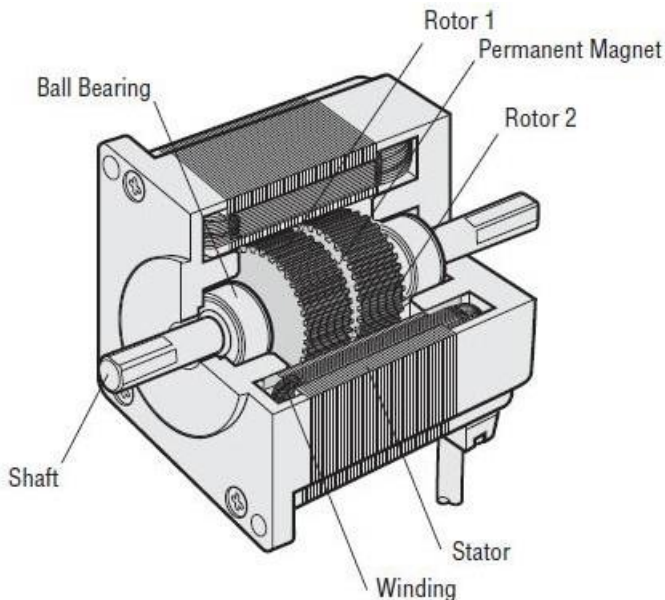
An advantage of the VR type stepper motor is that there is no need to change the polarity of the stator poles, so that its drive circuitry can be simplified. Its disadvantage is its inability for fine torque control since torque is proportional to the square of the current instead of to the

current. However, since it does not use permanent magnets, its high-speed performance is better than a PM type stepper motor.

VR type stepper motors have been around for a long time. These motors have less torque drop-off at higher motor speeds, so they are often a better choice than PM type stepper motors in mid to high speed applications. However, they are known to produce more noise, so their application range is limited. VR type stepper motors are less common than PM type stepper motors in the market.

### **Hybrid Type Stepper Motor**

A "hybrid" type stepper motor combines the design and advantages from both permanent magnet type and variable reluctance type stepper motors. Therefore, a hybrid type stepper motor uses both the permanent magnet rotor as well as a toothed rotor and stator in their design. With strong permanent magnets, toothed rotor, toothed stator, and a tiny air gap, a hybrid type stepper motor is able to focus the magnetic flux better than the other two types. Low loss is achieved by stacking magnetic steel laminations that can easily pass the magnetic flux.



Motor Structural Diagram: Cross-Section Parallel to Shaft

Figure 6.7: Hybrid Type Stepper Motor

The construction of a hybrid type stepper motor starts with two rotor cups (Rotor 1 and Rotor 2) and a strong rare earth permanent magnet which is axially magnetized. Two ball bearings mount the rotor into the motor casing. There are either 50 teeth ( $1.8^\circ$  per step) or 100 teeth ( $0.9^\circ$  per step) on the rotors. One rotor is magnetized as the North Pole, and one rotor is magnetized as the South Pole. Each tooth on the rotor cups becomes a magnetic pole.

Since there are 50 teeth, the full pitch is  $7.2^\circ$ . The two rotor cups are offset by a half pitch ( $3.6^\circ$ ) so the south pole teeth from rotor 1 line up in between the north pole teeth from rotor 2. From a cross-sectional view of the rotor, you can clearly see that the north and South Pole teeth are alternating because of the offset of the two rotor cups. When the windings are energized or excited by the driver, the stator poles turns into electromagnets, and the permanent magnet rotor follows them by both a pull and push effect and stops at fixed increments. The north poles from the stator will attract the south poles from the rotor, and vice versa.

There are eight stator poles in the stator. When windings are wound to the main poles and a current is applied, each pole is magnetized to the North Pole or the South Pole. Direction of current can determine the magnetic polarity. When excited, two poles at opposite sides have the same polarity, and two poles positioned at  $90^\circ$  from these poles have the opposite polarity. The main poles excited together are called "phases" and can be divided into two phases (phase A and phase B). This is why it's called a "two-phase" stepper motor.

The reason why hybrid type stepper motors rotate  $1.8^\circ$  per step is that the motor only moves a quarter of a tooth pitch per step due to the geometric design between the rotor and stator. When phase A is excited as the south pole and its stator teeth are directly aligned with the north pole teeth from the rotor, the stator teeth of phase B are actually offset from the teeth of the rotor by  $1.8^\circ$ . This is called the teeth arrangement offset and is the reason why a two-phase hybrid type stepper motor rotates  $1.8^\circ$  per step.

For a  $0.9^\circ$  per step stepper motor, both the rotor teeth need to increase to 100. Anything more than 100 teeth is quite difficult to manufacture.

With hybrid type stepper motors, high torque can be obtained by the rare earth permanent magnets while high resolution obtained by the small teeth is maintained. Also, the relationship between current and torque is close to proportional; making it easier to control than a VR type stepper motor. Hybrid type stepper motors can also achieve higher resolution (ie:  $0.72^\circ$  per full step / 500 steps per revolution). Even higher resolutions can be achieved by microstepping.

## Summary

- **PM Type:** permanent magnets in the rotor, moderate torque, low to mid-speed
- **VR Type:** toothed rotor/stator with ferromagnetic material, low torque, mid to high speed
- **Hybrid Type:** combines permanent magnets and teeth, good combination of torque and speed

The most popular stepper motors in the market are the hybrid type as it offers the best performance albeit at a higher cost. Hybrid type stepper motors will work well for most applications while PM type or VR type stepper motors are limited to certain applications. Stepper motor drivers are becoming increasingly smarter in recent years due to their technological improvements in functions, distributed control, and ease of programming. Gearheads and closed-loop feedback can be added to the stepper motor to expand its range of applications.

Thus, it is decided to proceed with hybrid stepper motors for our application due to requirement of a mix of speed and torque over the operational range in addition to widespread availability of the product in the market and thus it is easier to procure.

## Motor Specification

### Step Angle:

The step angle of a stepper motor is defined as the angle by which the rotor of a stepper motor moves when one input pulse is applied to the stator of the motor. The step angle is expressed in degrees. The step angle decides the resolution of positioning of a stepper motor i.e. smaller the step angle, the higher is the resolution of positioning of the motor.

The resolution or step number of a stepper motor is defined as the number of steps it makes in one revolution of the rotor, i.e.

$$\text{Resolution} = \frac{\text{Number of steps}}{\text{Number of revolutions of the rotor}}$$

Hence, if higher the resolution, the greater is the accuracy of positioning of objects by the stepper motor. The standard value for the stepper motor is  $1.8^\circ$ , as it ensures that there is a high resolution available. In addition, to obtain a value below  $1.8^\circ$ , microstepping will be needed to be done which will incur more cost thus the step angle of  $1.8^\circ$  is optimal for our usage.

## **Torque Requirement:**

Calculating the torque of the stepper motor:

$$\therefore \text{Torque} * \text{RPM} * 2\pi / 60 = F_{\text{axial}} * \text{velocity}$$

Also, Velocity = (RPM/60,000)

$$\therefore \text{Torque} * \text{RPM} * 2\pi / 60 = F_{\text{axial}} * \text{RPM} / 60,000$$

$$\therefore \text{Torque} = 0.64 \text{N-m}$$

Using this torque as the reference the motor was selected with suitable rpm.

Thus, Stepper motor of torque more than 0.64Nm needed to be selected.

## **Connection:**

The **unipolar stepper motor** operates with one winding with a center tap per phase. Each section of the winding is switched on for each direction of the magnetic field. Each winding is made relatively simple with the commutation circuit, this is done since the arrangement has a magnetic pole which can be reversed without switching the direction of the current. In most cases, given a phase, the common center tap for each winding is the following; three leads per phase and six leads for a regular two-phase stepper motor.

You will usually see that both these phases are often joined internally, this makes the stepper motor only have five leads. Often a stepper motor controller will be used to activate the drive transistors in the proper order.

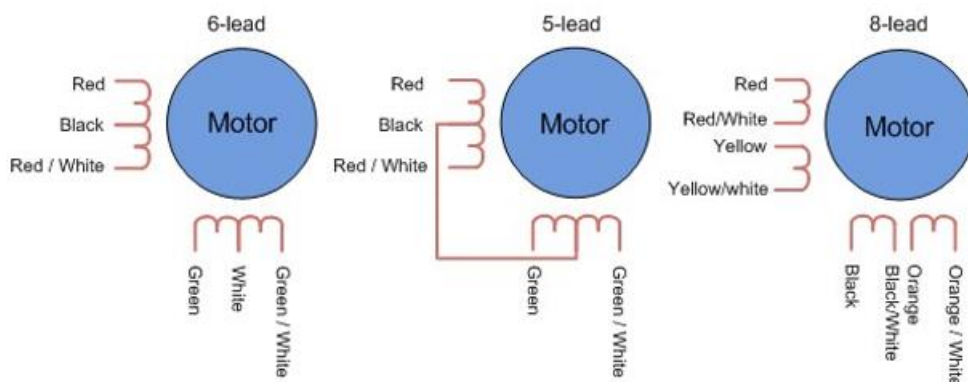


Figure 6.8: Unipolar Stepper Motor

With **bipolar stepper motors**, there is only a single winding per phase. The driving circuit needs to be more complicated to reverse the magnetic pole, this is done to reverse the current in the winding. This is done with an H-bridge arrangement, however, there are several driver chips that can be purchased to make this a simpler task. Unlike the unipolar stepper motor, the bipolar stepper motor has two leads per phase, neither of which are common. Static friction effects do happen with an H-bridge with certain drive topologies, however, this can be reduced by dithering the stepper motor signal at a higher frequency.

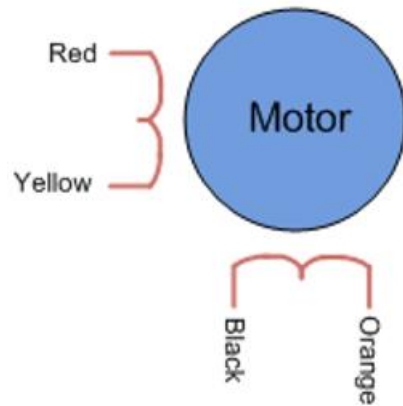


Figure 6.9: Bipolar Stepper Motor

Bipolar motors are generally better than unipolar motors. They have more torque and are more efficient. However, they are more complicated to drive because they need reverse current.

In terms of construction, bipolar motors have multiple (at least two) independent windings. A wire comes out of each of the winding's ends, so you get two wires per winding.

Unipolar motors also have multiple windings, however, in addition to the ends of each winding being connected to wires, the middle is also connected to a third wire. The absence of this third wire means that bipolar motors are slightly simpler to make. When it comes to driving these motors, however, the simpler bipolar motor requires a more complex driver. This is because, to precisely control its motion, we need to be able to drive current in each winding in both directions.

On the other hand, in a unipolar motor, we can get away with current that flows only in a single direction. This means that the driver electronics can be made simpler. The trade-off is that we use only half of each winding coil at a given time, and this translates to lower torque and efficiency.

However, with easy access to motor drivers like H-bridges, it is easy to drive bipolar motors with alternating current. Unipolar motors' advantage of not needing the reverse current is not a big deal anymore.

Furthermore, a stepper motor may be wired in either series or parallel, depending on the needs of the application. A series-wired motor will deliver more stall torque, but torque drops quickly as velocity increases. A parallel-wired motor typically maintains its (lower-than-series) torque to a higher velocity. Thus, bipolar parallel connection in the stepper motors seems like a better option.

As the main governing criterion for the Stepper motors are the ones mentioned above thus:

Step angle	1.8°
Holding Torque	> 0.64N-m
Connection	Bipolar parallel

Table 6.2: Stepper motor characteristics

As there is no constraints for space so the frame Dimension are not kept as the governing criterion. Thus based on the above points, the stepper motor decided for the actuation is 5618L-52P, NEMA 17.



Figure 6.10: 5618L-52P, NEMA 17.

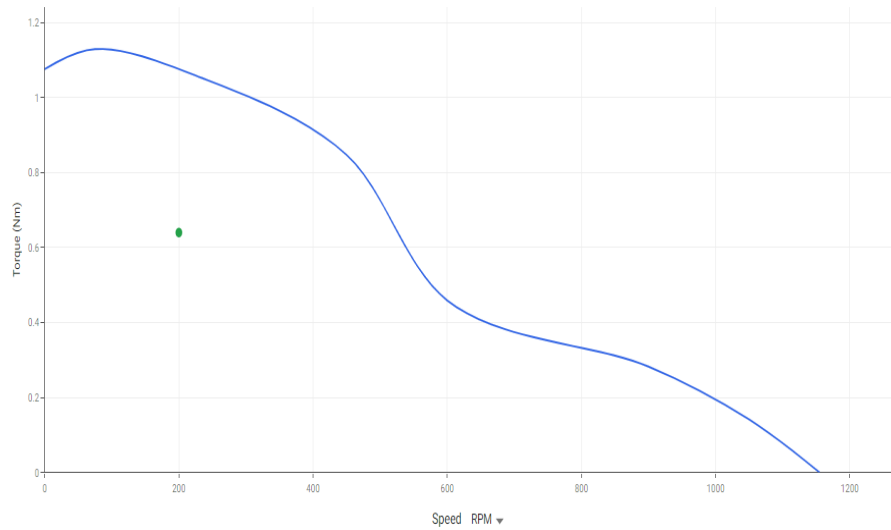


Figure 6.11: Torque Curve of 5618L-52P, NEMA 17

It can be observed from the above torque vs rpm curve of our stepper motor that the required motor torque is easily attainable in the operational range of 100-300 rpm.

<b>Motor Specifications</b>	
<b>Part Number</b>	5618L-52P
<b>Step Angle</b>	1.8°
<b>Frame Size</b>	57.20 mm
<b>Body Length</b>	77.00 mm
<b>Current (AMP)</b>	4.34 AMP
<b>Holding Torque</b>	1.24 Nm
<b>Resistance</b>	0.6
<b>Rotor Inertia</b>	219.49 g-cm <sup>2</sup>
<b>Number of leads</b>	4
<b>Connection</b>	Parallel

Table 6.3: Motor specifications

<b>Operating Specifications</b>	
<b>Radial Play</b>	0.03 mm @ 0.45 kg
<b>End Play</b>	0.08 mm @ 1.36 kg
<b>Shaft Run Out</b>	0.05 TIR
<b>Concentricity of Mounting Pilot to Shaft</b>	0.08 TIR
<b>Dimension "K"</b>	13.97 mm
<b>Max Axial Load</b>	5.90 kg
<b>Maximum Case Temperature</b>	80 °C maximum
<b>Ambient Temperature</b>	-20 ° to 50 °C
<b>Magnet Wire Insulation</b>	Class B 130 deg C
<b>Insulation Resistance</b>	100M Ohm at 500 VDC
<b>Dielectric Strength</b>	500 VDC for 1 min

Table 6.4: Operating specifications of motor

## 6.2 MICROCONTROLLER SELECTION

To control the logical, algorithmic and control function of the machine, a Microcontroller is used. It is like small computer with fixed amount of RAM and storage space. To perform control function and to apply PID control loop we need to use microcontroller.

Based on our requirements, we reviewed 3 microcontroller boards in the market:

- Arduino Nano RP2040
- Teensy 3.5
- ESP 32- S2

### Arduino Nano RP 2040:

The Arduino Nano RP2040 is an Arduino microcontroller board based around the RP2040 microcontroller created by Raspberry Pi. This is the same microcontroller processor used on the Raspberry Pi Pico, but this board includes built in networking using WiFi and Bluetooth BLE. This is provided using a onboard ESP32 through the ubloc NINA-W102. The board also has a 16MB SPI memory chip (AT25SF128A). It includes a 6-axis accelerometer (Inertial Measurement Unit) based around the (LSM6DSOXTR). It also includes a microphone (MP34DT05).

This does cost considerably more than the Raspberry Pi Pico, but it also includes many more features. It's also in a much smaller package.

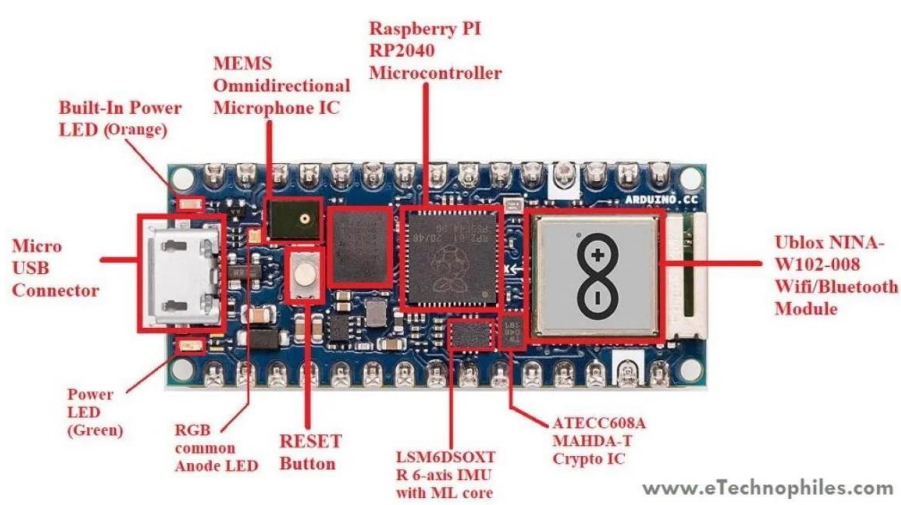


Figure 6.12: Arduino Nano RP 2040

## Teensy 3.5:

PJRC have developed a USB development board using a 32-bit 120 MHz ARM Cortex-M4 processor with floating point unit. Version 3.5 of this board, named “Teensy”, has the added benefit of 5V tolerance on all pins. This board is open-source, inexpensive, heavily documented, and includes an MCU that is much more powerful compared to the MCU’s of most official Arduino boards.

The MK64FX512 MCU that is featured by the Teensy 3.5 has two embedded 2-channel Flex-Timer modules. The encoder module operates by reading raising and falling edges from two encoder phase inputs. This will benefit real-time hardware quadrature decoding by alleviating the concern of needing to use interrupts to increment or decrement the encoder counter each time a pulse is received from the encoder and will not require any additional hardware.

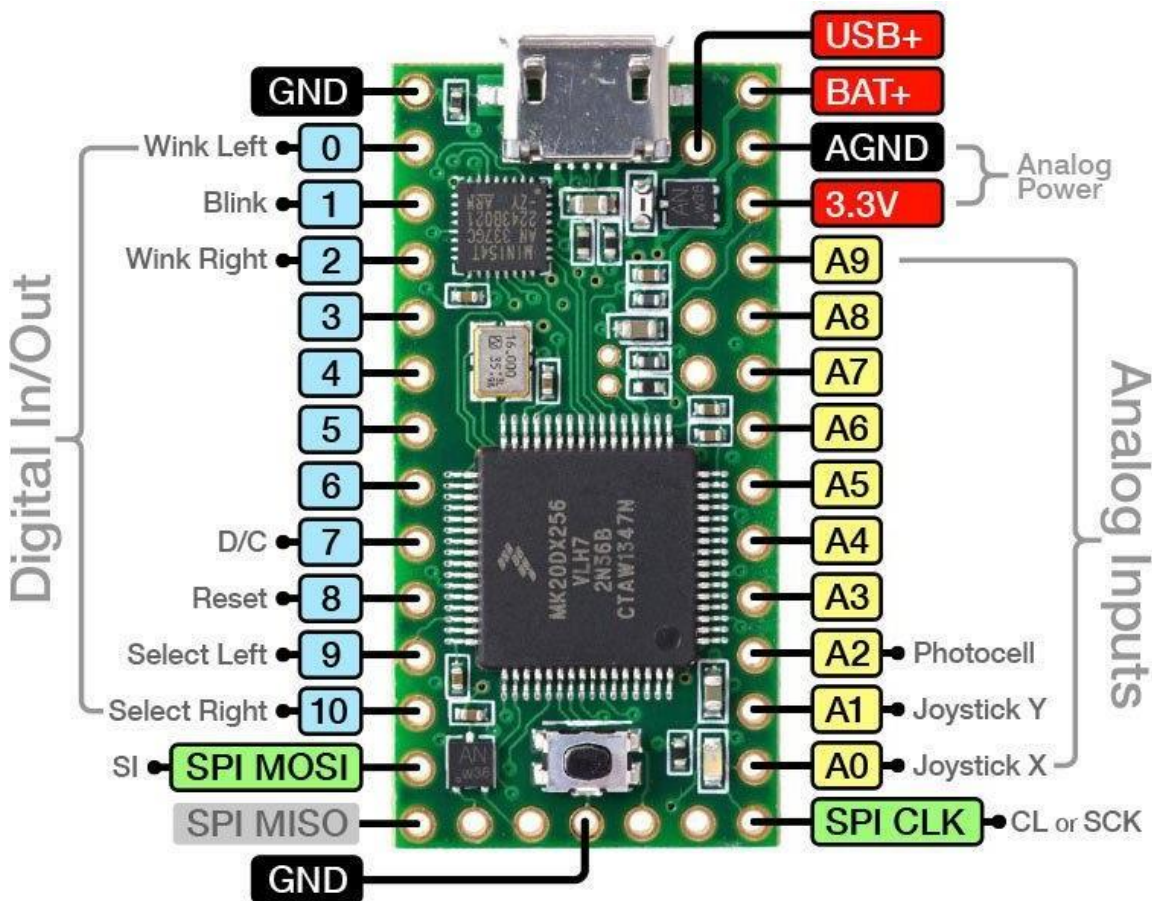


Figure 6.13: Teensy 3.5

## ESP32-S2:

ESP32-S2 a single core Wi-Fi microcontroller is designed by ESPRESSIF and featured with high performance, low power consumption, and a vast array of I/O (inputs and outputs). An integrated product featuring extremely low power consumption and 2.4 GHz WIFI on a system-on-chip solution makes it ideal for IoT applications. The Wi-Fi solution is offered by this chipfully complies with the IEEE 802.11b/g/n protocol. There is a32-bit Xtensa®LX7 processor on this chip that operates at 240MHz. This device has a rich set of peripheral interfaces including I2S, I2C, UART, SPI interface, LED PWM, LCD, camera interface, ADC touch sensor, DAC and temperature sensor, in addition to 43 GPIOs (General Purpose Inputs and Outputs). In addition, it supports full-speed USB On-The-Go (OTG), which allows USB communications.

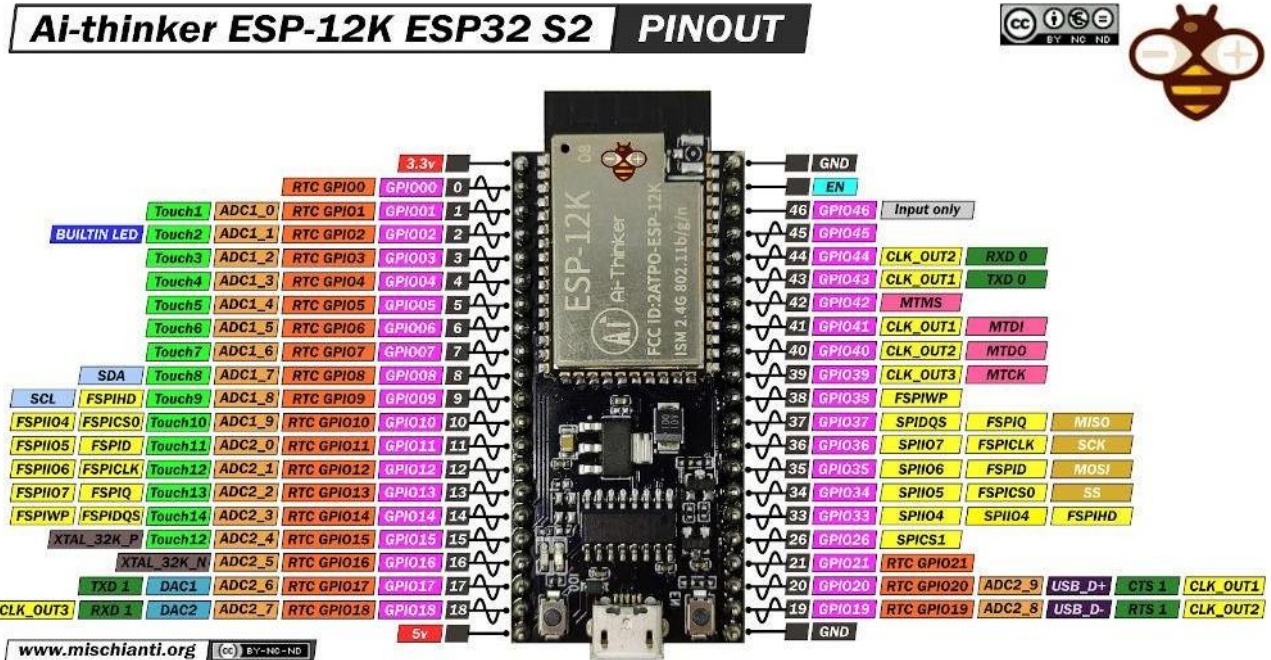


Figure 6.14: ESP32 S2

### **Microcontroller Selection Matrix:**

<b>Controller</b>	<b>Ease of Use</b>	<b>Documentation</b>	<b>Language</b>	<b>Performance</b>	<b>Auxiliary Features</b>	<b>Total Score</b>
Arduino Nano RP2040	5	3	1	5	4	18
Teensy 3.5 (ARM Cortex M4)	5	4	1	3	4	17
<b>ESP32-S2</b>	<b>5</b>	<b>4</b>	<b>1</b>	<b>5</b>	<b>4</b>	<b>19</b>

Table 6.5: Microcontroller selection matrix

Thus based on the above comparison, it is evident that ESP32-S2 is a better choice as it boast better performance, documentation although it may not have the as wide array of peripherals as the NANO RP 2040 but it has enough for the utility of this project, in addition, it is the cheapest of all the other options and thus widely available in the market. Furthermore, the compatibility of ESP32 package with the Arduino IDE makes it very easy to use the module for application.

### **6.3 PROGRAMMING LANGUAGE SELECTION**

Currently there exists a wide selection of microcontrollers on the market, each with different processors, uses, and features. The majority of microcontrollers are programmed in EmbeddedC/C++, while some of the newer experimental boards can run interpreted languages such as MicroPython. An understanding of the implications of using a compiled language such as Embedded C/C++ rather than an interpreted language such as MicroPython is very important when considering the design, development, and operation of the completed system.

In the tables below the benefits and drawbacks of coding in Embedded C/C++ and MicroPython are addressed, respectively.

<b>Embedded C/C++</b>	
<b>Pros</b>	<b>Cons</b>
Very fast/efficient. Up to 2 orders of magnitudes faster than interpreted languages.	No real-time debugger.
Compiled language.	More code required for same functionality
Typed language.	Very complex memory management.

Table 6.6 Pros and cons of Embedded C/C++

MicroPython	
Pros	Cons
Very easy to read and write.	Interpreted language – Up to 2 orders of magnitudes slower than a compiled language.
Real-time debugger.	Untyped language.
REPL (Read-eval-print loop).	

Table 6.7: Pros and Cons of MicroPython

The benefit to coding in MicroPython is the drastic simplification in code writing and readability. However, the performance of the interpreted language is orders of magnitude poorer compared to the more robust, compiled C/C++ language. Thus, Going for Embedded C/C++ is a better choice.

## 6.4 SENSORS USED

### 6.4.1 HALL EFFECT SENSOR

A Hall Effect sensor is a magnetic proximity sensor that is switched “ON” when a radially aligned magnetic field is applied to it. A Hall Effect sensor is a solid-state sensor i.e. it has no moving part in it. It is made up of semiconductors with a continuous current flowing through it when a magnetic field is applied across it the charged particle changes direction according to polarity. The separation of charged particles produces the Hall Effect circuit and once the output voltage is greater than the switching threshold the sensor turn “ON”.

This sensor will be used for obtaining the various positional inputs of Primary sheave, secondary sheaves.



Figure 6.15: 55505-00-02-A

### 6.4.2 STEPPER MOTOR LIMITER

Limit switches and homing sensors are ways of determining the position of either the stepper motor shaft itself or of the mechanism that the shaft is powering.

Both schemes use switches of some sort that are activated when the shaft or mechanism reaches a certain position.

Limit Switches are generally used in pairs and are placed at the mechanisms the end of travel. Once the switch is activated the motor will respond, how it responds is entirely up to you, but in most cases, it will either stop or reverse.

This component will be used to keep the stepper motor in within bounds with respect to the axial travel actuation along the lead screw, and acts a stopper at both the ends of the travel.



Figure 6.16: SS-5GL13T-A12

### 6.4.3 THERMOCOUPLE

A thermocouple is a sensor that measures temperature. It consists of two different types of metals, joined together at one end. When the junction of the two metals is heated or cooled, a voltage is created that can be correlated back to the temperature. A thermocouple is a simple, robust and cost-effective temperature sensor used in a wide range of temperature measurement processes.

When two wires composed of dissimilar metals are joined at both ends and one of the ends is heated, there is a continuous current which flows in the thermoelectric circuit. If this circuit is broken at the center, the net open circuit voltage (the Seebeck voltage) is a function of the junction temperature and the composition of the two metals. Which means that when the junction of the two metals is heated or cooled a voltage is produced that can be correlated back to the temperature.

This sensor is to be used for obtaining the temperature data for the cvt operation, which can be used to future analysis and tuning or formulation of strategy of keeping the temperature of cvtas low as possible to keep the performance efficiency as high as possible and also to safeguard the system to overheat and avoid the situation of burning of the CVT Belt.



Figure 6.17: 13461 Contactless IR

#### 6.4.4 IR SENSOR

IR sensor is an electronic device that emits the light in order to sense some object of the surroundings. An IR sensor can measure the heat of an object as well as detects the motion. The emitter is simply an IR LED (Light Emitting Diode) and the detector is simply an IR photodiode. Photodiode is sensitive to IR light of the same wavelength which is emitted by the IR LED. When IR light falls on the photodiode, the resistances and the output voltages will change in proportion to the magnitude of the IR light received.



Figure 6.18: Turnigy TGY-APD02

#### 6.4.5 POTENTIOMETER

A potentiometer consists of a three-terminal resistor and a moving contact, all of which form an adjustable voltage divider. These devices form one component of (typically) analog electronics, and their name comes from the fact that they serve as a voltage divider that varies electrical potential.

These devices feature a small handle that can slide either horizontally or vertically – depending on installation – to control the point of contact between the wiper and the resistor.

By putting an array of slide pots next to each other, it's easy to compare the levels visually. This quality is why you'll typically see linear pots in soundboards and graphic equalizers. The visual appearance of the array of sliders translates easily into a working idea of the tonal effect created.

Here the device will be used to realise the throttle response from the drive in terms to voltage to the circuit.



Figure 6.19: PTA6043-2015DPA103

SENSOR LIST		
Microcomputer	ESP32-S2	Control system integration
Hall effect sensor	55505-00-02-A	Position Encoder
Stepper motor Limiter	SS-5GL13T-A12	Lead Screw movement limiter
Thermocouple	13461 Contactless IR	Temperature sensing
IR sensor	Turnigy TGY-APD02	Optical Velocity encoder
Potentiometer	PTA6043-2015DPA103	Throttle response input

Table 6.8: Sensor List

## 6.5 SCHEMATIC DIAGRAM

The schematic for the electronic control system is dependent upon the microcontroller used and the number of and placement of the sensors that we use. A microcontroller with sufficient general purpose input and output pins for each sensor will allow each sensor to be wired (and therefore accessed) in parallel. With this configuration, each encoder, if configured in quadrature configuration, will correspond to two general input pins. If we do not implement the quadrature configuration, then each encoder will only require one general input pin. Each actuator will accordingly have some position/velocity sensor, and therefore will each need an additional one or two input pins. Each actuator will also need a limit switch to serve as the zero datum if we are not using an absolute position encoder. This yields a total of ten independent input pins required for the four encoders in quadrature configuration with two contact limit switches.

The ideal actuator driver will only require two pins per actuator – one to act as the enable pin and the other to send a pulse-width modulated signal to control the speed of the actuator. Since our final design has two different actuators, then we will need two general output pins and two pulse-width modulation (analog) pins which will be connected to a driver connecting the motor and the microcontroller.

Lastly, a thermocouple sensor will require one analog input pin to record the temperature inside the transmission, and the SDA and SCL pins can be used to control the heads up display in the driver's cockpit using the inter-integrated circuit protocol. Any additional sensors or controller input/output can be wired to any remaining pins or can be connected in parallel to the inter-integrated circuit bus. A schematic showing our initial electronic control system is shown below in Figure below.

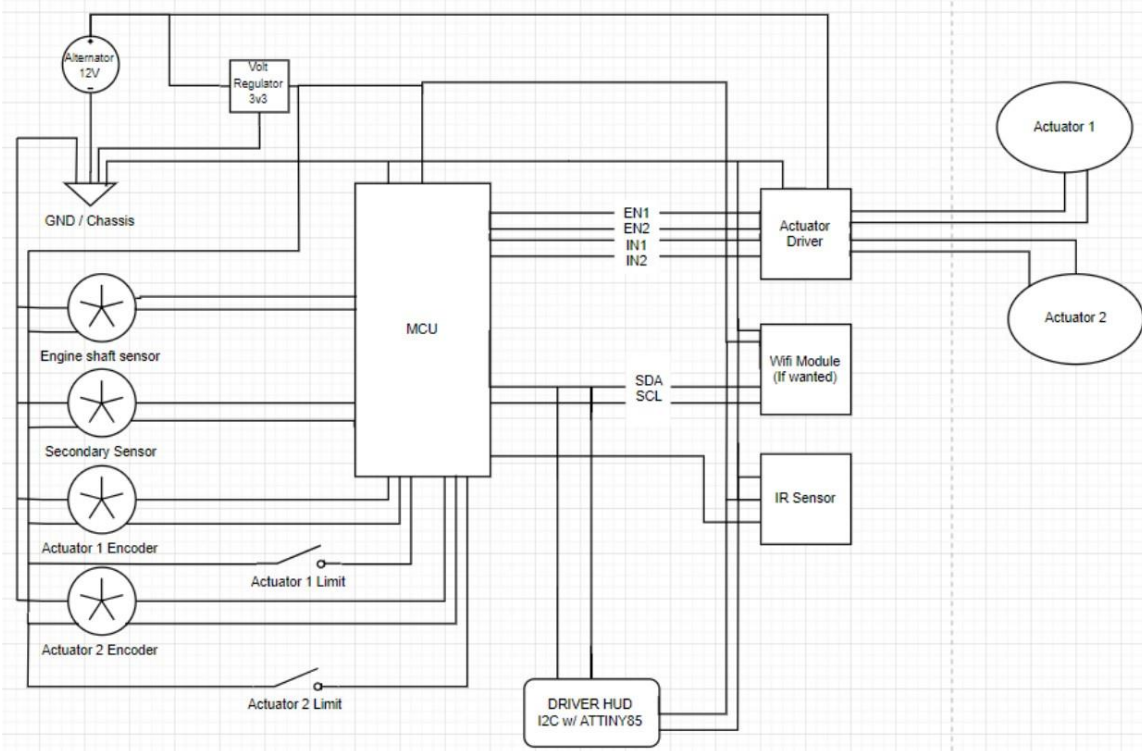


Figure 6.20: Schematic Diagram

This blow up is the initial design which underwent many changes and thus corresponding circuit is created in the design given below with major importance given to IR sensors and Thermocouple arrangements with ESP32-S2. Additionally, a circuit was realised in the KICAD software and developed so that it can be used to develop a custom PCB board if needed in the future.

The need for a custom PCB board helps in the packaging of the entire Control system and keeps it organized so that it is easier for servicing and debugging the circuit very efficiently. Thus even the replacement of the board will not pose an issue at the time of maintenance and servicing.

## 6.6 ELECTRICAL SYSTEM

The electrical system for the final design will follow the circuit schematic in Figure 24. This schematic was generated in KICAD and can easily be implemented on a custom PCB in the future if necessary.

The circuit schematic for the ESP32 controller board. Each component of the electronic system has been sized and selected to be well within their specifications with respect to voltage, signal quality and process ability, and heat dissipation. For instance, the MCU was chosen specifically for its 5V pin tolerance despite its 3.3V logic level.

The datasheets of each component were carefully read and understood to ensure that all inputs and outputs that we expect are in compliance with the allowable input and output range. Software development will follow test-driven development (TDD) procedures to improve the probability of success and to guarantee that during each feature addition, update, or patch that the software remains in compliance with our test specifications. As additional control algorithms are implemented, through the unit test framework and TDD we can guarantee that existing algorithms and system stability remain unbroken.

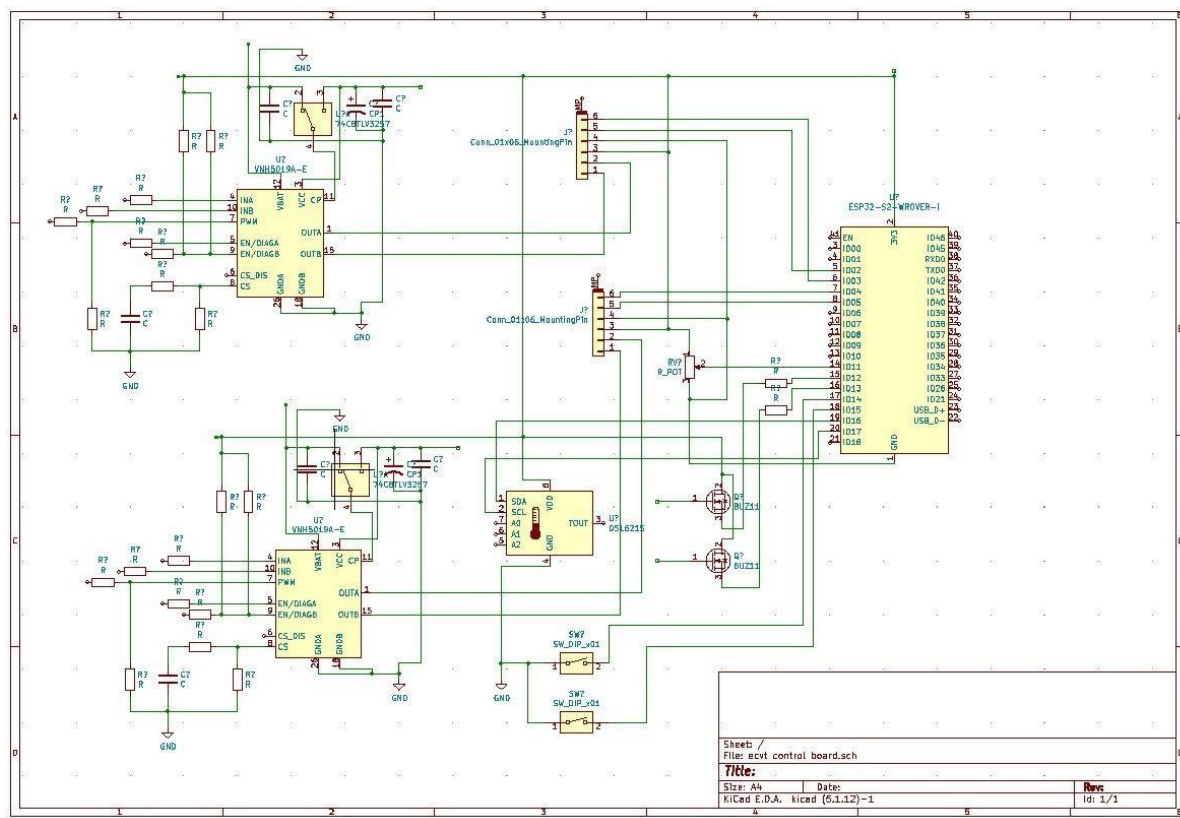


Figure 6.21: Circuit diagram of the Electrical system

# CHAPTER 7

## CONTROL SYSTEM CONCEPT DESIGN DEVELOPMENT

### 7.1 CONTROL SYSTEM DESIGN

Several control algorithms were researched, with a few simulated, to figure out which controller design would work best for this system.

#### PID controller

PID controllers are the most common type of control algorithm that is taught in an introductory course to controls and are an industry standard. The basic control architecture for a PID controller is shown in Figure xx. PID controllers are commonly used for systems that have a single actuator controlling a single state in the system. However, PID controllers can also be used to control multiple states with a single actuator or multiple states with several actuators. PID controllers are commonly used for systems that have a single actuator controlling a single state in the system. However, PID controllers can also be used to control multiple states with a single actuator or multiple states with several actuators.

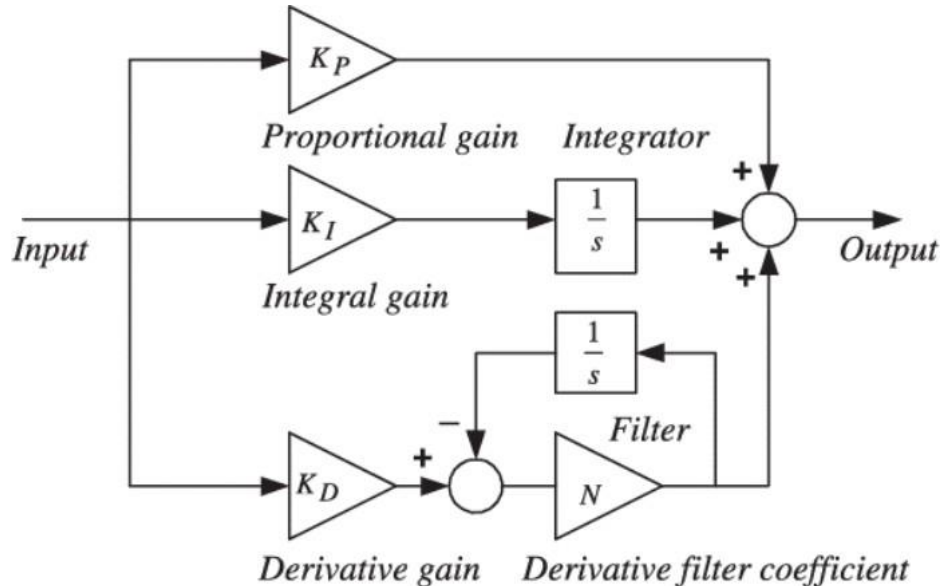


Figure 7.1: Basic Proportional-Integral-Differential Controller Architecture

**Pros:** PI controllers are easy to design, intuitive control action, easy to implement in hardware and easy to tune.

**Cons:** PI controllers are only guaranteed to work for linear systems, not robust.

## Fuzzy Logic

Fuzzy logic removes the math from a standard control algorithm and controls the system solely based upon user-programmed logic. The basic control architecture for a fuzzy logic controller is shown in Figure xx. A fuzzy logic controller is designed from the user's deductive reasoning of how the actuator should control the system's state based on the current sensor inputs. Because fuzzy logic control is designed based on user intuition, a fuzzy logic controller is not designed based upon a mathematical model of the system. It is easy to make a bad fuzzy logic control. However, because of a fuzzy logic controller's degrees of freedom, it is possible to build a functional controller.

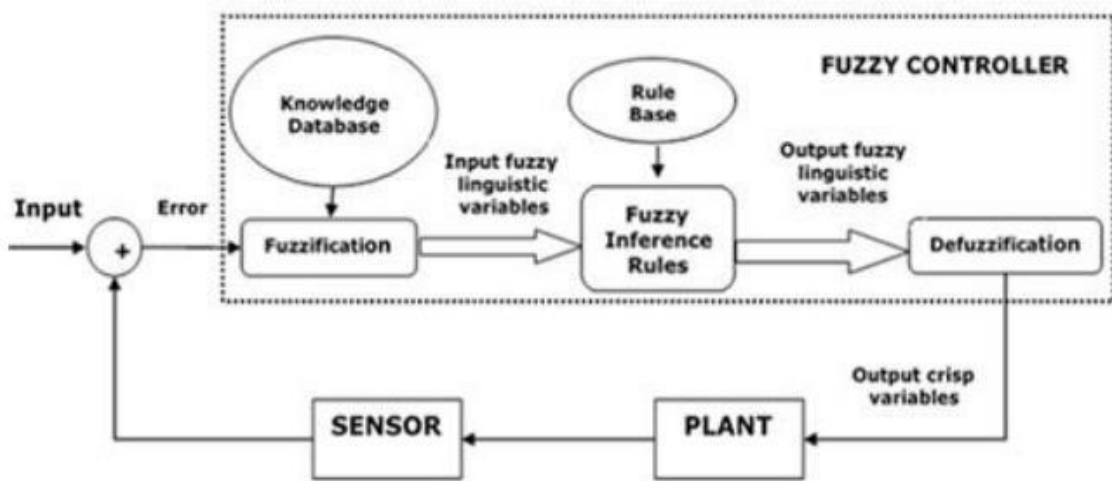


Figure 7.2: Fuzzy Logic Controller Architecture

**Pros:** A model of the plant is not required to design the controller, lots of design freedom to make a robust control.

**Cons:** Very difficult to tune, not designed to be optimal with respect to the system state or input, difficult to program

## Optimal Control/ FSFB

Optimal control and full state feedback (FSFB) are lumped in the same control algorithm category because optimal control uses the same feedback principle as FSFB, but optimal control is used to design optimal FSFB gains based upon minimizing some cost function relating to the plant. The basic control architecture for FSFB is shown in Figure xx. FSFB is used primarily to control multi-input-multi-output (MIMO) systems. FSFB feedbacks the state of the system that when multiplied by the feedback gain,  $k$ , the system's eigenvalues become negative real parts. Optimal control uses mathematical analysis to pick an 'optimal'  $K$  gain that minimizes some desired variable of the system. FSFB is used primarily to regulate the system (drive the states to zero), but can also be used to track some input into the system.

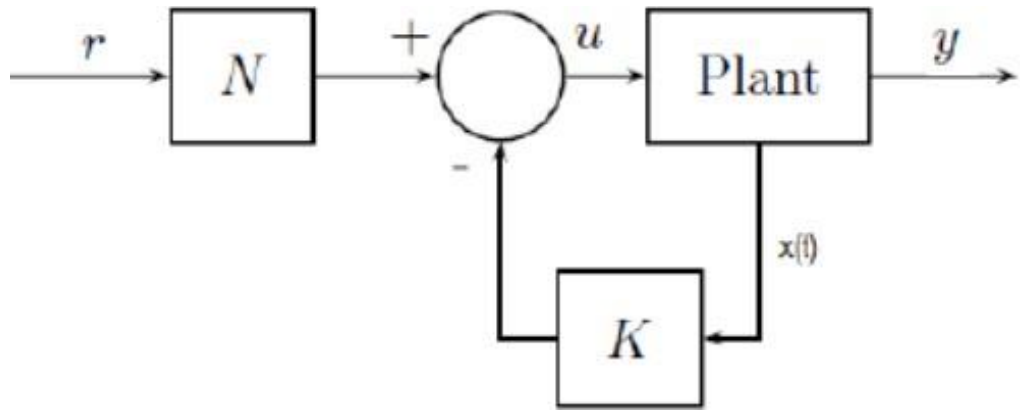


Figure 7.3: Optimal Control and Full State Feedback

**Pros:** FSFB is the best when trying to control multiple states, easy to implement in hardware, easy to tune.

**Cons:** Abstracts the intuition from the controller, not easy to design for performance requirements.

### Look up Table

A look up table is not a control algorithm; however, it could be a viable solution. Since an IC engine runs at peak power for a certain motor speed it is the case that a unique gear ratio of the CVT exists for every wheel speed. A plot of the Baja IC engine's power vs. engine rpm is shown in Figure 7.4.

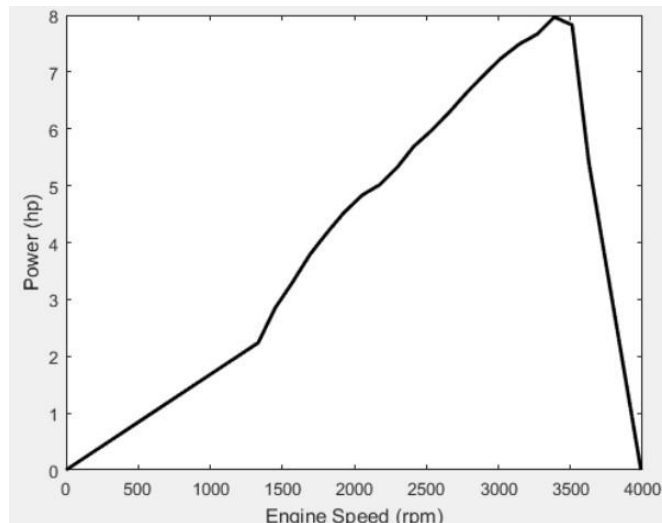


Figure 7.4: Baja Engine Power Curve

It is seen that the peak power output of Baja's IC engine when the engine's speed is at about 3400 rpm. Figure 7.5 shows the CVT's gear ratio vs. the wheel's rotational speed.



Figure 7.5: Ideal CVT Shift Curve

Figure 7.5 shows possibility of a look up table containing the ideal CVT gear ratio for every wheel rotational speed. The lookup table would be implemented in the hardware that controls the CVT.

**Pros:** The CVT gear ratio would theoretically be actuated to the ideal gear ratio for a given wheel rotational speed. Very simple to employ and understand.

**Cons:** The lookup table doesn't account for the time it takes to actuate the CVT to a desired gear ratio. The lookup table removes all 'intelligence' that a regular controller provides; the lookup table is only a function of wheel rotational speed and would not act differently if slip occurred between the pulleys and belts

### Neural Network

Neural Networks are a branch of controllers that are based upon artificial intelligence principles. Neural Networks control a given system by 'learning' what control inputs give a desired control output and which control inputs don't give a desired control output and adjusts the control algorithm accordingly. Figure 7.6 shows what a standard neural network control architecture looks like.

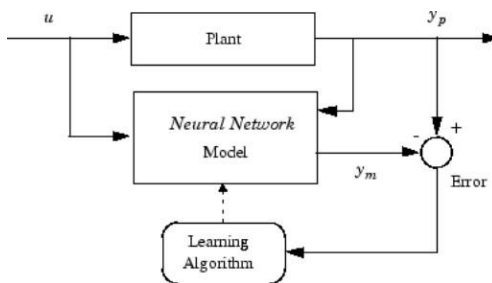


Figure 7.6: Neural Network Controller Model

**Pros:** Control system can adopt to new environments; which could be helpful for an off roading environment.

**Cons:** When mechatronics system turns on it takes time for the neural network to adjust to its environment. Neural networks do not guarantee convergence to a stable controller. Also we would never truly understand how CVT shifts are.

### Selection Matrix for the Control Algorithm

Controller	Tuning	Ease of designing	System Fit	Robustness	Programming	Total Score
<b>PID controller</b>	<b>5</b>	<b>3</b>	<b>3</b>	<b>1</b>	<b>2</b>	<b>14</b>
<b>Fuzzy Logic</b>	2	1	5	2	2	12
<b>FSFB</b>	4	2	0	1	2	9
<b>Look Up Table</b>	<b>5</b>	<b>3</b>	<b>4</b>	<b>0</b>	<b>2</b>	<b>14</b>
<b>Neutral Network</b>	2	0	4	1	0	7

Table 7.1: Selection matrix for control algorithm

Thus, based on the above selection criteria, PID controller and Look up Table are the two optimal options for the control logic algorithm but even among the two, PID controller is selected due to its higher robustness which is crucial to the utility of the component in adapting to the fast changing conditions.

## 7.2 CODE IMPLEMENTATION

Arduino IDE is used to develop the code for the hardware system as it helps to make the control more compatible to the existing circuit and actuators.

The code mainly focus on the principle equation of PID controllers, i.e.

$$u(t) = K_p e(t) + K_i \int e(t) dt + K_p \frac{de}{dt}$$

$u(t)$  = PID control variable  
 $K_p$  = proportional gain  
 $e(t)$  = error value  
 $K_i$  = integral gain  
 $de$  = change in error value  
 $dt$  = change in time

Figure 7.7: PID Equation

K<sub>p</sub>, K<sub>i</sub> and K<sub>d</sub> are decided based on various iteration runs in various conditions. Furthermore, keeping these variables user defined, provides a flexible approach to problem under observation. Thus, in the future if an altogether different situation arises then there is scope of optimization by changing the gain values.

After the gains are defined, various other parameters pertaining to the PID equation are found and calculating and plugged into the equation in order to optimize the rpm values of the CVT sheaves. Based on the values of the primary sheave the Secondary pulley rpm requirement is calculated again to formulate again using a relation between the Primary rpm belt length and secondary rpm. Thus the optimized values of the rpm at every instance of the operation is calculated.

```
#include <Wire.h>
#include <math.h>
#include <Servo.h>

Servo PrimMotor;
Servo SecMotor;

float k1=.5;
float k2=55;
float k3=.00001;

int k11[] = {2,4,6}; //Input the Prmactual value here for hardcoded
int k12[] = {};//Input the SensorActual value here for hardcoded

int milliOld;
int milliNew;
int dt;

float PrimTarget=0;
float PrimActual;
float PrimError=0;
float PrimErrorOld;
float PrimErrorChange;
float PrimErrorSlope=0;
float PrimErrorArea=0;
float PrimMotorVal=0;

float SecTarget=0;
float SecActual;
float SecError=0;
float SecErrorOld;
float SecErrorChange;
float SecErrorSlope=0;
```

Figure 7.8: Arduino Code Part 1

```

float SecErrorArea=0;
float SecMotorVal=0;

void setup() {
    // put your setup code here, to run once:
Serial.begin(115200);

delay(1000);

PrimMotor.attach(2);
SecMotor.attach(3);

PrimMotor.write(PrimMotorVal);
delay(20);
SecMotor.write(SecMotorVal);
delay(20);

milliNew=millis();
}

void loop() {
delay(1000);

//For hardcoding:
//PrimActual = k1[i];
//SecActual=k12[i]
//i++;

//For taking sensor realtime value use an if clause:
// if
//PrimActual= read(sensorA);
//SecActual= read(sensorB) ;
PrimActual=PrimActual/(2*3.141592654)*360;

```

Figure 7.9: Arduino Code Part 2

```

//SecActual= read(sensorB) ;
PrimActual=PrimActual/(2*3.141592654)*360;
SecActual=SecActual/(2*3.141592654)*360;

milliOld=milliNew;
milliNew=millis();
dt=milliNew-milliOld;

PrimErrorOld=PrimError;
PrimError=PrimTarget-PrimActual;
PrimErrorChange=PrimError-PrimErrorOld;
PrimErrorSlope=PrimErrorChange/dt;
PrimErrorArea=PrimErrorArea+PrimError*dt;

SecErrorOld=SecError;
SecError=SecTarget-SecActual;
SecErrorChange=SecError-SecErrorOld;
SecErrorSlope=SecErrorChange/dt;
SecErrorArea=SecErrorArea+SecError*dt;

PrimMotorVal=PrimMotorVal+k1*PrimError+k2*PrimErrorSlope+k3*PrimErrorArea;
PrimMotor.write(PrimMotorVal);

SecMotorVal=SecMotorVal+k1*SecError+k2*SecErrorSlope+k3*SecErrorArea;
SecMotor.write(SecMotorVal);

Serial.print(PrimTarget);
Serial.print(",");
Serial.print(PrimActual);
Serial.print(",");
Serial.print(SecTarget);
Serial.print(",");
Serial.print(SecActual);
Serial.print(",");
Serial.println(system);

```

Figure 7.10: Arduino Code Part 3

In addition, a python code is also developed to check the logic of the code by hardcoding the sensor input data in form of both primary and secondary pulley rpms. The input values in a string format datatype which are then treated as sensor data and thus the above logic and thus a test trail is conduction to check for the credibility of the logic and the results for which are mentioned below.

## **Iteration 1**

```

1 import time
2 import math
3
4 e = 50
5 l = 890
6 z = 500
7 rSec = 0
8 # Change these values only
9 primValue = [2600, 3400, 2900]
10 dt = 1000
11 PrimTarget = SecTarget = 3600
12 k1 = 0.5
13 k2 = 55.0
14 k3 = .00001
15
16 PrimError = PrimErrorArea = PrimMotorVal = 0
17
18 n = len(primValue)
19 for i in range(0, n):
20     time.sleep(1.0)
21     PrimActual = primValue[i]
22     PrimErrorOld = PrimError
23     PrimError = PrimTarget-PrimActual
24     PrimErrorChange = PrimError-PrimErrorOld
25     PrimErrorSlope = PrimErrorChange/dt
26     PrimErrorArea = PrimErrorArea+PrimError*dt
27
28     print(f'For iteration {i} :')
29
30     PrimMotorVal = PrimMotorVal+k1*PrimError+k2*PrimErrorSlope+k3*PrimErrorArea
31     print("Prime Motor move this many degrees: " + str(PrimMotorVal))

```

Figure 7.11: Python Code Iteration 1 Part 1

```

31 SecErrorOld = SecError
32 SecError = SecTarget-SecActual
33 SecErrorChange = SecError-SecErrorOld
34 SecErrorSlope = SecErrorChange/dt
35 SecErrorArea = SecErrorArea+SecError*dt
36
37 print(f'For iteration {i} :')
38
39 PrimMotorVal = PrimMotorVal+k1*PrimError+k2*PrimErrorSlope+k3*PrimErrorArea
40 print("Prime Motor move this many degrees: " + str(PrimMotorVal))
41
42 SecMotorVal = SecMotorVal+k1*SecError+k2*SecErrorSlope+k3*SecErrorArea
43 print("Secondary Motor move this many degrees: " + str(SecMotorVal))
44
45 print("Prime Target : " + str(PrimTarget))
46 print("Prime Actual : " + str(PrimActual))
47 print("Secondary Target : " + str(SecTarget))
48 print("Secondary Actual : " + str(SecActual))

```

Figure 7.12: Python Code Iteration 1 Part 2

```

44     print("Prime Target : " + str(PrimTarget))
45     print("Prime Actual : " + str(PrimActual))
46     print("Secondary Target : " + str(SecTarget))
47     print("Secondary Actual : " + str(SecActual))
48
49

```

PROBLEMS OUTPUT DEBUG CONSOLE TERMINAL

```

Prime Actual : 1950
Secondary Target : 0
PS C:\Users\User> & D:/anaconda3/python.exe "c:/Users/User/Desktop/BE project pr/Code Python test/code.py"
For iteration 0 :
Prime Motor move this many degrees: -270.0
Secondary Motor move this many degrees: -131.25
Prime Target : 0
Prime Actual : 1800
Secondary Target : 0
Secondary Actual : 875
For iteration 1 :
Prime Motor move this many degrees: -463.5
Secondary Motor move this many degrees: -232.5
Prime Target : 0
Prime Actual : 1650
Secondary Target : 0
Secondary Actual : 850
For iteration 2 :
Prime Motor move this many degrees: -724.5
Secondary Motor move this many degrees: -362.75
Prime Target : 0
Prime Actual : 1950
Secondary Target : 0
Secondary Actual : 980

```

Figure 7.13: Python Code Iteration 1 Part 3

## Iteration 2

There was another iteration conducted where the secondary and primary sheaves axial motion is calculated. Here the primary axial motion actuation is calculated by the PID loop optimization and secondary axial motion is dependent on the primary cvt motion actuation values based on the below three equations sequentially:

1.  $r_{primary} = r_{min,primary} + (LBW - a_p) / (2 * \tan 14)$
2.  $L = (r_{primary} + r_{secondary}) * \pi + (r_{secondary} - r_{primary}) * (2 * \sin^{-1}((r_{secondary} - r_{primary}) / A)) + 2 * (A^2 - (r_{secondary} - r_{primary})^2)^{1/2}$
3.  $R_{secondary} = r_{min,secondary} + (LBW - a_s) / (2 * \tan 14)$

Here,  $r_{min,primary}$  = Minimum radius of Primary Sheave

$r_{min,secondary}$  = Minimum radius of Secondary Sheave

$LBW$  = Lower Belt Width

$A$  = Centre to center distance

$a_p$  = primary axial distance

$a_s$  = Secondary axial distance

Here the axial motion of primary is obtained after the pid loop and then fed to the equation 1 as  $a_p$ , to obtain  $r_{primary}$ . Then which is used to obtain the value of  $r_{secondary}$  using a while loop for the second equation and under a bounded constraint. Finally,  $a_s$  is calculated from the third equation.

```

1 import time
2 import math
3
4 e = 50
5 l = 890
6 z = 500
7 rSec = 0
8 # Change these values only
9 primValue = [2600, 3400, 2900]
10 dt = 1000
11 PrimTarget = SecTarget = 3600
12 k1 = 0.5
13 k2 = 55.0
14 k3 = .00001
15
16 PrimError = PrimErrorArea = PrimMotorVal = 0
17
18 n = len(primValue)
19 for i in range(0, n):
20     time.sleep(1.0)
21     PrimActual = primValue[i]
22     PrimErrorOld = PrimError
23     PrimError = PrimTarget-PrimActual
24     PrimErrorChange = PrimError-PrimErrorOld
25     PrimErrorSlope = PrimErrorChange/dt
26     PrimErrorArea = PrimErrorArea+PrimError*dt
27
28     print(f'For iteration {i} :')
29
30     PrimMotorVal = PrimMotorVal+k1*PrimError+k2*PrimErrorSlope+k3*PrimErrorArea
31     print("Prime Motor move this many degrees: " + str(PrimMotorVal))

```

Figure 7.14: Python Code Iteration 2 Part 1

```

21 PrimActual = primValue[i]
22 PrimErrorOld = PrimError
23 PrimError = PrimTarget-PrimActual
24 PrimErrorChange = PrimError-PrimErrorOld
25 PrimErrorSlope = PrimErrorChange/dt
26 PrimErrorArea = PrimErrorArea+PrimError*dt
27
28 print(f'For iteration {i} :')
29
30 PrimMotorVal = PrimMotorVal+k1*PrimError+k2*PrimErrorSlope+k3*PrimErrorArea
31 print("Prime Motor move this many degrees: " + str(PrimMotorVal))
32 ap = PrimMotorVal*5/360
33 rPrime = 19.05 + ((14.44-ap)/0.498)
34 e = 50.0
35 while e <= 180:
36     dummy = rPrime*(math.pi-(2*math.asin((e-rPrime)/z))) + e*(math.pi +
37     (2*math.asin((e-rPrime)/z))) + 2*(math.sqrt((z**2)-((e-rPrime)**2)))
38     e = e + 0.0010
39     if dummy == 1:
40         rSec = e
41         print(rSec)
42         break
43     as1 = 44.0297 - 0.498*rSec
44     print(str(as1) + "In radians")
45     print(str(ap) + " in Radians")
46     SecMotorVal = 360 * as1 / 5
47     print("Prime Motor move this many degrees: " + str(SecMotorVal))
48     print("Prime Target : " + str(PrimTarget))
49     print("Prime Actual : " + str(PrimActual))
50

```

Figure 7.15: Python Code Iteration 2 Part 2

## CHAPTER 8

### SIMULATION

Using MATLAB Simulink we can simulate the entire process and find out results of operation. We have used MATLAB to simulate the mechanical and electrical components of the ECVT.

In the models below the ideology of the entire system is explained. Being divided into 2 different sub systems: controller subsystem and plant subsystem, a closed loop feedback setup is achieved, wherein the output of the controller block is the input for the plant block, and vice versa.

The major components considered are: Engine RPM, wheel RPM and CVT Ratio.

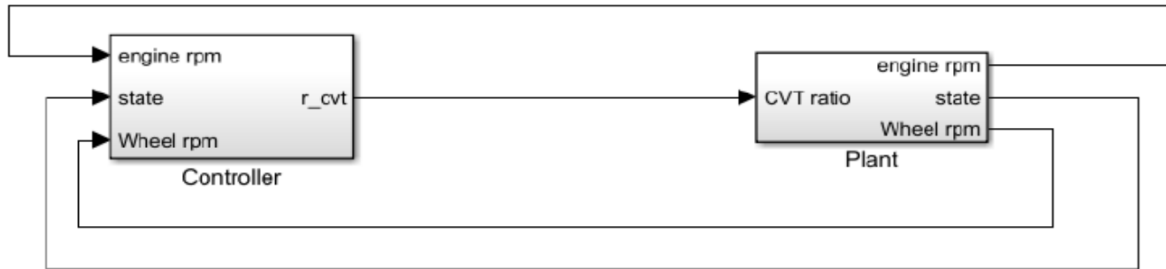


Figure 8.1: Modelling Ideology

The controller subsystem basically contains PID Model for optimizing CVT output RPM with respect to engine RPM. A function is provided to feed the engine RPM, the output of which is further fed into the PID controller. The output RPM sensor input is fed through another controller wherein the omega is obtained and through regression processes and  $r_{cvt}$  variable is obtained which is further processed along with the PID output in the variant source block and the final result is filtered and the final output is obtained. The state input is keeps a track of the status of the system below.

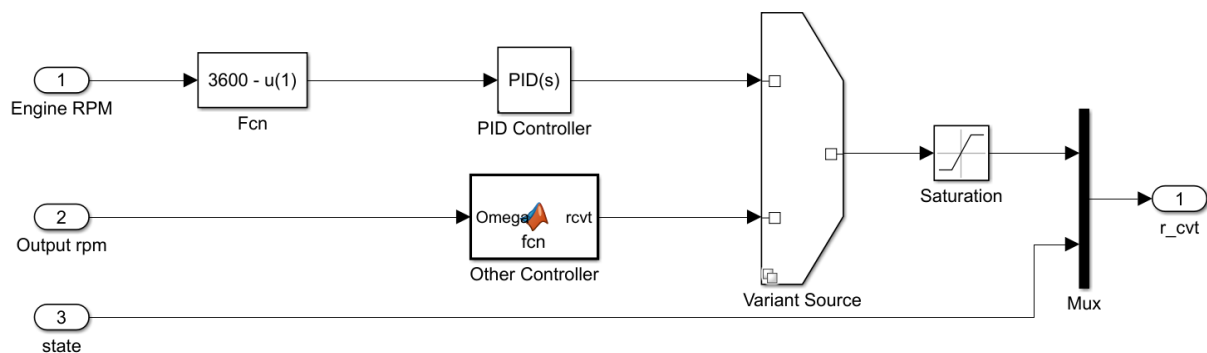


Figure 8.2: Controller Subsystem

The  $r_{cvt}$  variable from the previous block is then fed into the plant subsystem in the form of CVT\_ratio which is then demultiplexed into 2 inputs for the custom MATLAB function, the output of which is compared to the axial distance with optimized CVT\_ratio. There is a provision provided for the verification of the PID control in the form of dead zone branch from the first MATLAB function. A scope function will generate a graph of real time PID functioning. A lookup table visualization is obtained in the end, the output from which is sent to the workspace. After processing in the workspace, the values generated are run through MATLAB Baja CVT tuning model to simulate the operation of a CVT to the real life as accurately as possible. The graphs generated from this are mentioned below.

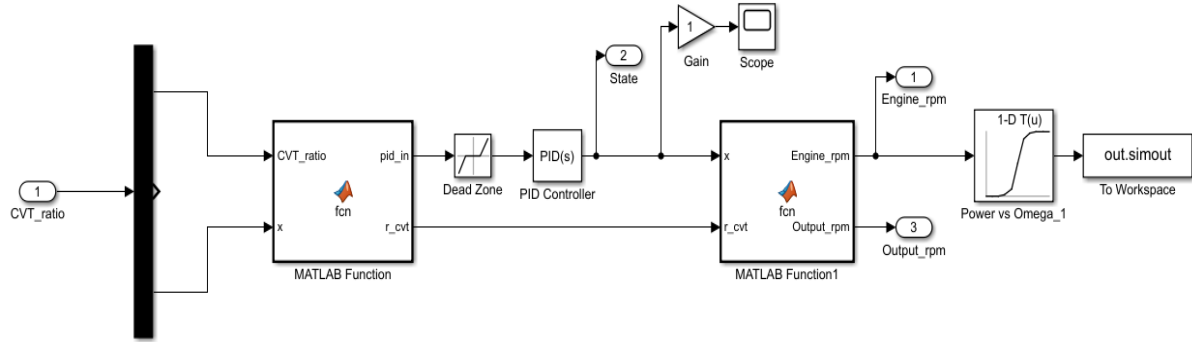


Figure 8.3: Plant Subsystem

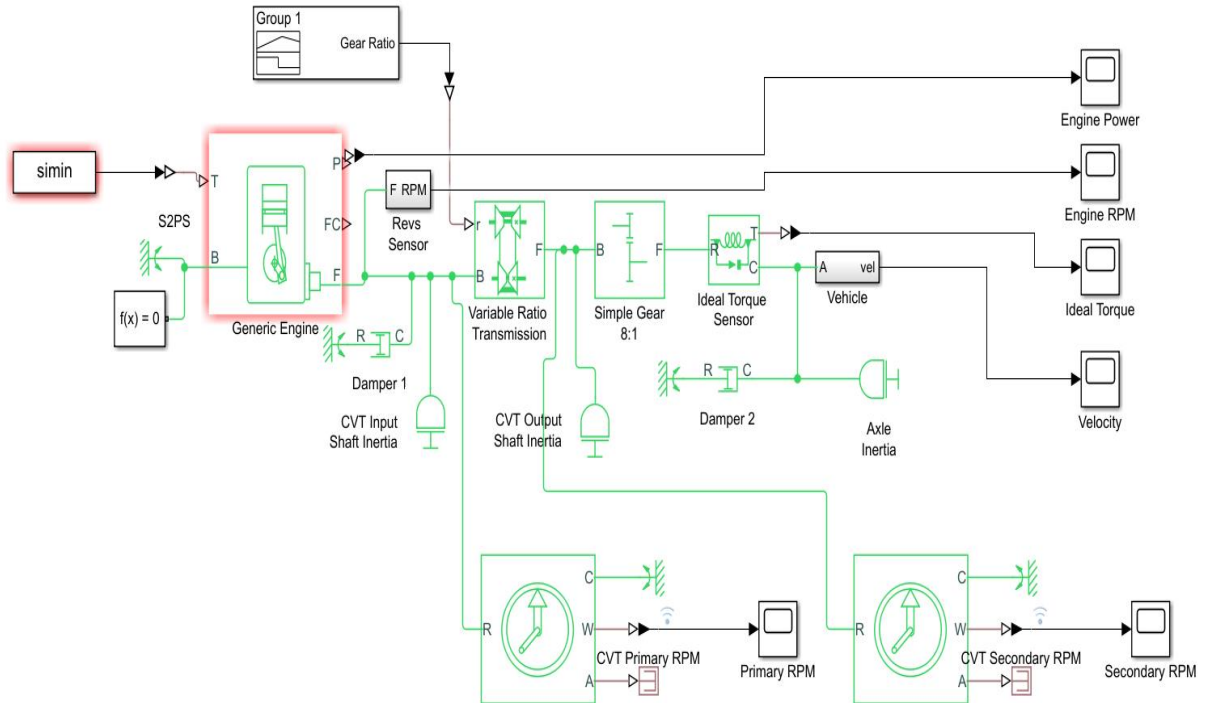


Figure 8.4: MATLAB-BAJA Model

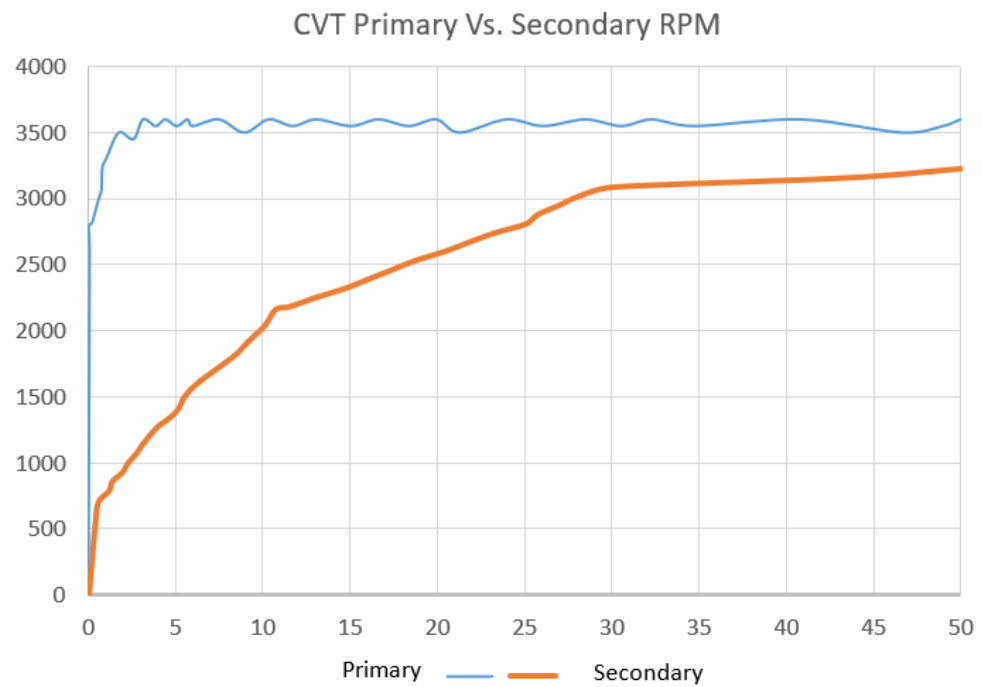


Figure 8.5: Primary and Secondary RPMs vs Speed (kmph)

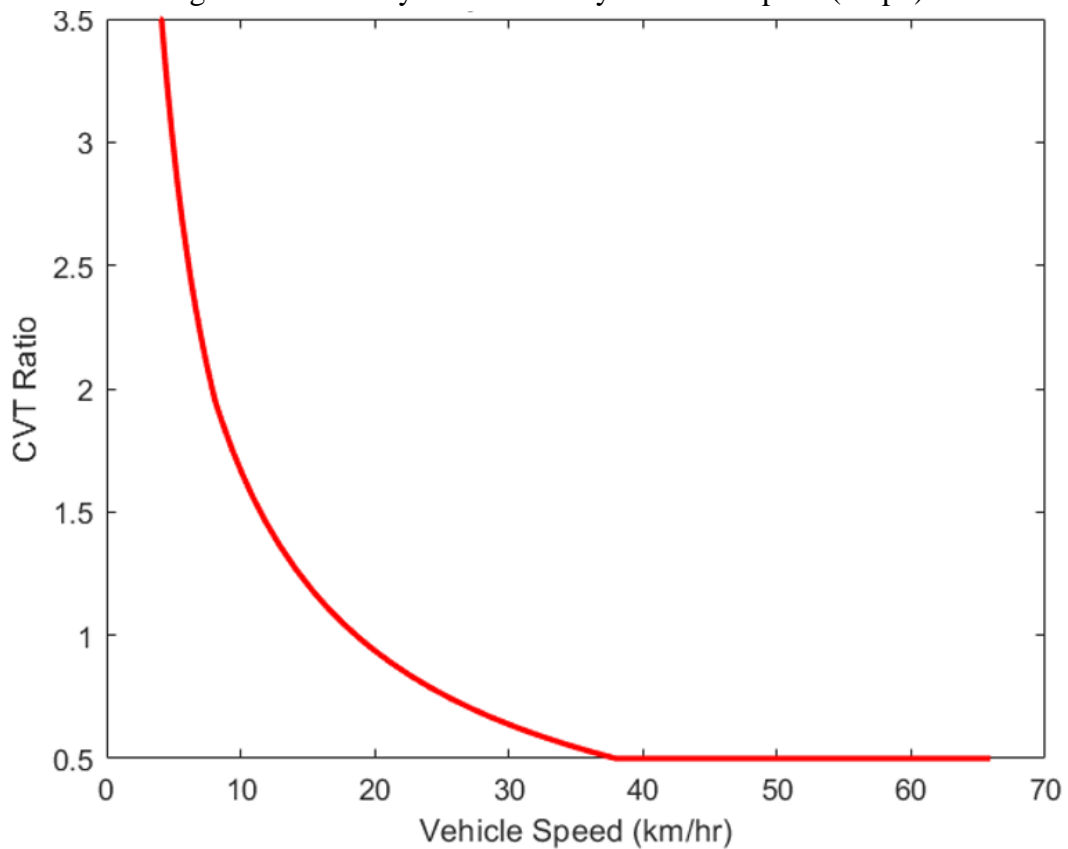


Figure 8.6: CVT Ratio vs Vehicle Speed (kmph)

## **CHAPTER 9**

## **FUTURE SCOPE**

The ECVT designed is lightweight, compact, efficient and gives more performance than the present mechanical CVT. However, there still scope for improvement in the control logic of the ECVT.

Futuristic technologies, such as Artificial Intelligence and Machine Learning can be incorporated and with the help of data, the tuning process can be optimised further, which would make the entire product more efficient.

Further research in the materials can be done to reduce the losses generated in the sheave and the wheel. Alloys which are lightweight, cost efficient and having lower heat conductivity can be used to reduce the losses thereby making the mechanical subsystem more efficient.

Although the losses generated due to heating have been greatly reduced, CFD analysis can be done for the entire enclosure, which would aid in further minimising the heat generated by the use if laminar flow inside the CVT casing.

## **CONCLUSION**

Today's mechanical CVTs in All Terrain Vehicles incur high losses, low ease of assembly and usage with very high costs. The ECVT designed in this project work has resulted in high efficiency, high strength, very high ease of assembly and usage with much lower costs for various applications. Selection of various components and sensors has been done keeping efficiency, weight as well as cost in mind. The designed ECVT also has a much higher overall shift ratio, which results in higher performance during pickup as well as during acceleration. Based on the FEA results and electronic components selection, the design is future proof and it can be concluded that the CVT is not prone to failure in the given working parameters. The entire assembly is lightweight, compact and has increased life over the conventional mechanical CVT.

## **REFERENCES**

- [1] Supriyo, Bambang & Tawi, K. & Jamaluddin, Hishamuddin. (2013). Experimental study of an electro-mechanical CVT ratio controller. International Journal of Automotive Technology. 14. 10.1007/s12239-013-0035-x.
- [2] Selan, Vishnu. "Analysis, Design and Application of Continuously Variable Transmission (CVT)." *International Journal of Engineering Research and Applications* 5 (2015): 99-105.
- [3] Ryu, W. & Kim, Hong Sup. (2008). CVT ratio control with consideration of CVT system loss. International Journal of Automotive Technology. 9. 459-465. 10.1007/s12239-008-0055-0.
- [4] Aulakh, Deepinder. (2017). Development of simulation approach for CVT tuning using dual level genetic algorithm. Cogent Engineering. 4. 10.1080/23311916.2017.1398299.
- [5] Bhandari, V., 2010. *Design of machine elements*. New Delhi: Tata McGraw-Hill.
- [6] Xie, F. & Wang, J. & Wanga, Y.. (2011). Study on CVT Ratio Tracking Controller. Procedia Engineering. 16. 723-728. 10.1016/j.proeng.2011.08.1147.
- [7] Akehurst, S., Parker, D. A., and Schaaf, S. (October 3, 2005). "CVT Rolling Traction Drives—A Review of Research Into Their Design, Functionality, and Modeling." ASME. *J. Mech. Des.* September 2006; 128(5): 1165–1176. <https://doi.org/10.1115/1.2214737>
- [8] Dong, Jian & Dong, Zuomin & Crawford, Curran. (2011). Review of Continuously Variable Transmission Powertrain System for Hybrid Electric Vehicles. 10.1115/IMECE2011-63321.
- [9] Srivastava, N., and Haque, I. (September 28, 2006). "Transient Dynamics of the Metal V-Belt CVT: Effects of Pulley Flexibility and Friction Characteristic." ASME. *J. Comput. Nonlinear Dynam.* January 2007; 2(1): 86–97. <https://doi.org/10.1115/1.2389233>
- [10] Bin Feng, G. Gong and Huayong Yang, "Self-tuning-parameter fuzzy PID temperature control in a large hydraulic system," 2009 IEEE/ASME International Conference on Advanced Intelligent Mechatronics, 2009, pp. 1418-1422, doi: 10.1109/AIM.2009.5229854.
- [11] Carbone, G., De Novellis, L., Commissaris, G., and Steinbuch, M. (January 22, 2010). "An Enhanced CMM Model for the Accurate Prediction of Steady-State Performance of CVT Chain Drives." ASME. *J. Mech. Des.* February 2010; 132(2): 021005. <https://doi.org/10.1115/1.4000833>
- [12] Shukla, Prakash & Tiwari, Prashant & Singh, Yashwant & Singh, Vikas. (2017). Design and Performance Study of Continuously Variable Transmission (CVT). International Journal of Engineering Research and. V6. 10.17577/IJERTV6IS040668.

[13] Wang, Yubin & Cheng, Ming & Chau, K.T.. (2009). Review of Electronic-continuously Variable Transmission Propulsion System for Full Hybrid Electric Vehicles. Journal of Asian Electric Vehicles. 7. 1297-1302. 10.4130/jaev.7.1297.

[14] Shubham Upadhyaya, "*Study of different types of continuous variable transmission for an electric hybrid vehicle*" SSRG International Journal of Mechanical Engineering 7.6 (2020): 47-54. Crossref, <https://doi.org/10.14445/23488360/IJME-V7I6P108>

[15] Ruan J, Walker PD, Wu J, Zhang N, Zhang B. Development of continuously variable transmission and multi-speed dual-clutch transmission for pure electric vehicle. Advances in Mechanical Engineering. February 2018. doi:10.1177/1687814018758223